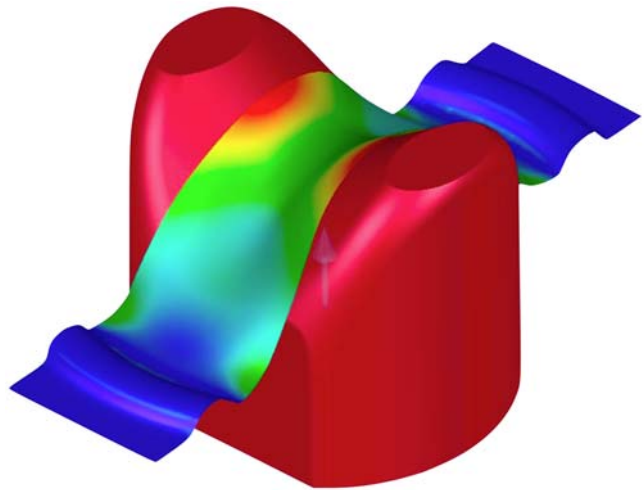

Master's Degree Thesis Mechanical Engineering

Fracture prediction of stretched shear cut edges in sheets made of Dual-Phase steel



Johannes Falk

*Department of Mechanical Engineering
Blekinge Institute of Technology, Karlskrona, Sweden 2017*

Supervisor: Mats Sigvant, Ph.D, Technical Expert, Volvo Cars

Assistant supervisor: Johan Pilthammar, M.Sc, CAE Engineer & Ph.D. Candidate, Volvo Cars

ABSTRACT

Dual-Phase (DP) steels, part of the group of Advanced High Strength Steels (AHSS), are used by car manufactures due to its large strength to weight ratio. The high strength of the DP steel does have a negative impact on the formability during sheet metal forming and stretch forming, e.g. fractures often appear in shear cut edges during forming of blanks made of DP steel.

The main objective with this thesis is to develop a new punch for Volvo Cars that concentrates the strain to the sheared edges of a test specimen made from different types of DP steel. This is done to be able to measure and obtain maximum fracture strain during stretch forming tests in a press. The newly developed test method is called CTEST (Concentrated Trim Edge Strain Test).

The tests are performed with DP steel specimens with three different qualities of the shear cut edges; fine cut, medium cut and worn cut. DP steels tested are DP600GI, DP600UC and DP800GI from three different suppliers. 10 different types of DP steels are tested in this study with different thickness. Thickness of specimens tested are 1 mm, 1.1 mm, 1.5 mm and 2 mm and all specimens tested have a lengthwise (RD) rolling direction.

The quality of the sheared cut edge has a great impact to the formability and maximum fracture strain of the specimen. A specimen with a fine cut endures higher fracture strain than medium cut and a worn cut for all types of DP steel with different thickness. A 1 mm thick specimen endures a lower fracture strain than 1.5 mm and 2 mm specimen for all cut qualities.

Further, the impact of the orientation of the burr zone of a shear cut edge is studied. With the burr zone facing upwards from the CTEST punch the formability of the specimens is decreased compared to a burr zone facing downwards, especially for a worn cut specimen with micro cracks and imperfections in the edge surface.

ARAMIS Digital Image Correlation (DIC) system is used to analyze the specimen edges during press experiments. The ARAMIS results unveil that several small fractures appear in the sheared edges of a specimen just before the specimens split into two pieces. This phenomenon was seen for specimen with worn and medium shear cut qualities.

Finite Element (FE) simulations of the CTEST is performed in AutoForm to determine maximum values of the true strain for the three different cut qualities. The simulation in AutoForm does show a slightly higher value of the force and press depth than the value from the press test before maximum fracture strain is reached. The small fractures seen in ARAMIS just before the specimen split into two pieces cannot be seen in the simulation in AutoForm.

SAMMANFATTNING

Dual-Phase (DP) stål klassas som ett höghållfast stål och används av biltillverkare på grund av hög hållfasthet relativt vikten. Den höga hållfastheten har dock en negativ inverkan på formbarheten under plåtformning och sprickor uppkommer ofta under formningsprocessen av DP stål.

Det huvudsakliga syftet med detta examensarbete är att utveckla och designa en ny stämpel för Volvo Cars som, under tester i press, koncentrerar töjningen till klippta kanter på en provbit tillverkad av DP stål. Detta görs för att möjliggöra mätning av maximal töjning innan brott på klippkanterna. Den nyutvecklade stämpeln och provmetoden heter CTEST (Concentrated Trim Edge Strain Test).

CTEST utförs i en press med provbitar av DP stål med tre olika kvalitéter på de klippta testkanterna; fint klipp, mellanklipp och dåligt klipp. DP stålen som testas i studien är DP600GI, DP600UC och DP800GI från tre olika stålleverantörer. Provbitarnas tjocklek är 1 mm, 1.1 mm, 1.5 mm och 2 mm. Totalt testades 10 olika typer av DP stål och samtliga provbitar som testas hade en längsgående valsriktning relativt klippkanterna.

Kvaliteten på klippkanterna på provbitarna har stor inverkan på formbarheten innan brott. En provbit med en fin klippkant klarar av ett djupare pressdjup och en högre stämpelkraft än en provbit med mellan och dålig kvalitet på klippkanterna. Lägst formbarhet innan brott har provbitar med dåliga klippkanter och detta gäller för samtliga ståltjocklekar testade. Provbitar med en tjocklek på 1 mm har en lägre formbarhet innan brott än provbitar med en tjocklek på 1.5 mm och 2 mm.

Även inverkan av orienteringen av klippgraden på formbarheten undersöks i denna studie. Med klippgraden vänd uppåt relativt CTEST stämpeln, har provbitarna en lägre formbarhet än om klippgraden är vänd ner mot stämpeln. Detta fenomen synd tydligast för provbitar med dåliga klippkanter i vilka graden innehåller småsprickor.

ARAMIS som är ett digitalt bildkorrelationsprogram, används för att analysera provbitarna och göra mätningar av töjningen från presstesterna. Analysen av resultatet i ARAMIS visar att flera små sprickor uppkommer längs den klippta kanten hos provbitarna innan maximalt pressdjup och maximal stämpelkraft uppnås. Vid maximalt pressdjup och maximal stämpelkraft är det en av dessa småsprickor som växer till en stor spricka, vilket leder till att provbiten delas. Detta fenomen var tydligast för provbitar med dåliga och mellan klippkvaliteter.

Simuleringar av presstesterna gjordes i AutoForm för att bestämma maximala värden för sann töjning för respektive klippkvalité och materialtyp. Simuleringen i AutoForm visar något högre värden på stämpelkraft och pressdjup för provbitarna innan maximal sann töjning uppnås än vad värdena från presstesterna i ARAMIS visar. De små sprickorna som upptäcktes innan maximalt pressdjup och maximal stämpelkraft i experimenten kan inte ses i simuleringen i AutoForm.

ACKNOWLEDGEMENT

This Master's Degree Thesis was carried out at Volvo Cars Body Components, Olofström, Sweden, and at the Department of Mechanical Engineering, Blekinge Institute of Technology (BTH) from September 2016 to January 2017 under the supervision of Dr. Mats Sigvant and doctoral candidate Johan Pilthammar. This Master's Degree Thesis is an outcome from the master program, Mechanical Engineering 2012 at the Department of Mechanical Engineering at BTH.

First, I would like to express my sincere gratitude and appreciation to supervisor Ph.D. Mats Sigvant, Volvo Cars, who has, with his great ambition and expertise, guided and supported me throughout the project. I am also thankful to my assistant supervisor Johan Pilthammar, Volvo Cars, for his words of advice and support. I would also like to express my deepest gratitude to Volvo Cars Body Components (VCBC) for sponsoring me with material and software but also a big thank to all other staff at VCBC who have supported me and contributed with ideas and valuable feedback.

A great thank you to my examiner Dr. Ansel Berghuvud, BTH, who has provided me with valuable and essential information during the project. Many thanks to all staff at Swerea IVF, Olofström, for helping me with the tests and for manufacturing and preparation of all test material.

At last, I would like to thank my family and classmates who have helped and supported me in the work of making a substantial work.

Karlskrona, January 2017

Johannes Falk

NOMENCLATURE

Notations

<i>Symbol</i>	<i>Description</i>
A_i	Cross-section area of specimen
d	Cut clearance
S	Engineering Stress
e	Engineering strain
ε	True strain
μ	Friction Coefficient

Acronyms

<i>AHSS</i>	Advanced High Strength Steel
<i>CAD</i>	Computer Aided Design
<i>CTEST</i>	Concentrated Trim Edge Strain Test
<i>FE</i>	Finite Element
<i>DP</i>	Dual Phase
<i>DIC</i>	Digital Image Correlation
<i>FLC</i>	Forming Limit Curve
<i>GI</i>	Galvanized steel
<i>HEC</i>	Hole Expanding Test
<i>KRE</i>	Edge Fracture Sensitivity Test (Kanten Riss Empfindlichkeitstest)
<i>RD</i>	Rolling direction
<i>SET</i>	Sheared Edge Tensile test
<i>SETi</i>	Sheared Edge Tensile test improved
<i>SPA</i>	Scalable Production Architecture
<i>TD</i>	Transverse Direction (Rolling)
<i>UC</i>	Uncoated steel
<i>VCBC</i>	Volvo Cars Body Components

TABLE OF CONTENT

ABSTRACT

SAMMANFATTNING

ACKNOWLEDGEMENT

1 INTRODUCTION

1.1 Introduction	1
1.2 Background.....	1
1.3 Objectives	2
1.4 Delimitations	2
1.5 Thesis questions.....	3

2 THEORETICAL FRAMEWORK

2.1 Dual-Phase (DP) steel.....	4
2.2 Shear cutting of metals	5
2.3 Sheet metal forming	8
2.4 Strain.....	9
2.6 AutoForm simulation software.....	10
2.7 ARAMIS measuring system.....	10
2.8 Profilometer	11
2.9 Rolling and rolling direction	11
2.10 Galvanizing of steel.....	12
2.11 Related work.....	12

3 METHOD

3.1 Project approach	14
3.2 Study of literature and related research	14
3.3 Tensile tests	15
3.4 Design of the punch geometry.....	15
3.5 Materials tested.....	17
3.6 Cut edges of specimens	20
3.7 Radius measurement of cutting tool edges	21
3.8 Pre-tests	23
3.9 Experimental tests	25
3.10 Comparison and evaluation of results	27

3.10.1	Compilation of results in Excel.....	27
3.10.2	Simulation in AutoForm.....	28
3.10.3	Evaluation of press experiments in ARAMIS.....	33
3.10.4	Comparison of geometry of simulation and ARAMIS	33

4 RESULTS

4.1	Tensile tests	34
4.2	Design of the punch geometry.....	35
4.3	Cut edges of specimens	36
4.3.1	Worn cut - worn tool and 20 % clearance.....	36
4.3.2	Medium cut - fine tool and 20 % clearance	39
4.3.3	Fine cut - worn tool and 5 % clearance.....	41
4.4	Radius measurement of cut tool edges	44
4.4.1	Worn cut tool.....	44
4.4.2	Fine cut tool before cut operation	44
4.5	Pre-tests	45
4.6	Influence of rolling direction.....	45
4.7	Influence of burr zone orientation	46
4.8	Results from the press experiments.....	47
4.8.1	DP600GI 1 mm different suppliers	48
4.8.2	DP600GI 1.5 mm different suppliers	49
4.8.3	DP600GI 1.5 mm vs. DP600GI 2 mm Supplier A.....	50
4.8.4	DP600GI vs. DP600UC Supplier A.....	51
4.8.5	DP600GI 1 mm vs. DP800GI 1 mm Supplier B.....	52
4.8.6	DP600GI 1.5 mm vs. DP800GI 1.5 mm Supplier B.....	53
4.9	Evaluation of press experiments in ARAMIS	54
4.10	Comparison of simulation in AutoForm vs. ARAMIS DIC system	55
4.10.1	Comparison of geometry of simulations and ARAMIS DIC system.....	55
4.10.2	At maximum punch force and punch depth	55
4.10.3	Punch force vs. punch depth curve.....	57
4.10.4	New values of maximum fracture strain for simulations in AutoForm	58

5 DISCUSSION

5.1	Design of the punch geometry.....	59
5.2	Tensile tests	59
5.3	Cut edges of specimens	59
5.3.1	Worn cut - worn tool and 20 % clearance.....	59

5.3.2 Medium cut - fine tool and 20 % clearance	60
5.3.3 Fine cut - worn tool and 5 % clearance.....	60
5.4 Radius measurement of cutting tool edges.....	60
5.5 Pre-tests	60
5.6 Influence of rolling direction.....	60
5.7 Influence of burr zone orientation	61
5.8 Results from the press experiments.....	61
5.8.1 DP600GI 1 mm thick from different suppliers	61
5.8.2 DP600GI 1.5 mm thick from different suppliers	61
5.8.3 DP600GI 1.5 mm thick vs. DP600GI 2 mm thick Supplier A.....	61
5.8.4 DP600GI vs. DP600UC Supplier A.....	61
5.8.5 DP600GI 1 mm thick vs. DP800GI 1 mm thick Supplier B.....	62
5.8.6 DP600GI 1.5 mm thick vs. DP800GI 1.5 mm thick Supplier B.....	62
5.9 Evaluation of press experiments in ARAMIS	62
5.10 Comparison of simulation in AutoForm vs. ARAMIS DIC system	62
5.10.1 Comparison of geometry of simulations and ARAMIS DIC system.....	62
5.10.2 At maximum punch force and punch depth	62
5.10.3 Punch force vs. punch depth curve.....	63
5.10.4 New values of maximum fracture strain for simulations in AutoForm	63
6 CONCLUSIONS.....	64
7 RECOMMENDATIONS AND FUTURE WORK.....	65
8 REFERENCES.....	66
APPENDIX A.....	67

LIST OF FIGURES

Figure 1.1. A fracture in a shear cut edge of a DP steel body part. 2

Figure 2.1. The martensitic (white) and ferrite (grey) microstructure of DP steel. 4

Figure 2.2. The steel body structure of the 2015 Volvo XC90. The marked out parts are examples of parts made of DP steel. 5

Figure 2.3. The different zones for a shear cut edge. 6

Figure 2.4. With optimal adjustments, the fractures will meet and give a fine cut. When the edge approaches approx. 40% (0.4t) of the thickness of the material a fracture will appear. 6

Figure 2.5. With a large clearance between the shear edges, the fractures won't meet up and this will result in worse cut quality. 7

Figure 2.6. Worn edges of the cut tool leads to greater zone of deformation and the fracture will appear later. 8

Figure 2.7. Sheet metal forming with the die components. 8

Figure 2.8. Stretch forming. 9

Figure 2.10. FE-simulation in AutoForm. 10

Figure 2.11. The two cameras of the ARAMIS system determine changes of the test specimen during a tensile test or similar tests. 10

Figure 2.12. The Surfascan measurement system used for measurement of edge geometry in this study. 11

Figure 2.13. The microstructure of the steel changes during the rolling operation. 11

Figure 3.1. A visual schedule over the phases in the current project. 14

Figure 3.2. The automatic tensile test machine used for the tensile tests. Dog bone specimens ready for testing can be seen down in the middle. 15

Figure 3.3. Modelling of punch in Catia V5. 16

Figure 3.4. The three different geometries of the punch that was created in Catia V5 and analyzed in AutoForm. 16

Figure 3.5. The figures present the major strain distribution for the specimen from the simulation using two different designs of the punch. 17

Figure 3.6. The polished edge of all specimens was prepared in an automatic grinding machine. 18

Figure 3.7. A test specimen before cut procedure. 19

Figure 3.8. A finished test specimen after cut procedure. 19

Figure 3.9. A test specimen with one polished and one cut edge. This type of specimen was used during both the pre-test and experimental tests. 20

Figure 3.10. The microscope used to analyze the cut quality of the edges. 20

Figure 3.11. The edge radius was measured in five different positions of the tool edge. 21

Figure 3.12. The Surfascan probe during measurement of worn cut tool. 22

Figure 3.13. A projection of the fine edge from the Surfascan measuring program. 22

Figure 3.14. Installation of the CTEST punch in the press. 23

Figure 3.15. The painted test specimen was placed in the press and later formed until the maximum tensile strain was exceeded. The same test method was used for the experimental tests.....	24
Figure 3.16. A specimen before the press operation.	25
Figure 3.17. A specimen after the press operation. The fracture can be seen at the top of the specimen.	26
Figure 3.18. The press used for all tests. The two computers used for measuring can be seen in front of the press. One computer was used to measure forces and punch depth and the other computer was used for the ARAMIS DIC system.	27
Diagram 3.1. The type of force/punch depth diagram used for comparison of result between simulation and real test. All results were also presented using this type of diagram.	28
Figure 3.20. An overview of the die, binder, punch and specimen used for the simulation. The same type of tools was used during the physical press tests.	28
Figure 3.21. The gap at bottom was adjusted for each specimen type to the same distance as where the real test specimen did break from the main tests.....	29
Figure 3.22. Material data for each supplier and type of steel was changed for every new type of specimen simulated.	29
Figure 3.23. The maximum edge strain was edited and adjusted for each specimen tested to get the edge crack value as close to 1 as possible.....	30
Figure 3.24. The “edge crack” function in AutoForm presents where on the specimen there is a risk for fractures and thereby where the highest strain can be found. All values over 1 means that a fracture will appear.	31
Figure 3.25. The friction coefficient was set to 0.1 for the simulation in AutoForm.....	32
Figure 4.1. The CTEST punch.	35
Figure 4.2. FE-simulation of the final design of punch. The left picture presents the risk of edge crack and the right picture presents the major strain.....	35
Figure 4.3. The worn cut edge of 1 mm DP600GI specimen from Supplier A.....	36
Figure 4.4. The worn cut edge of 1.5 mm DP600GI specimen from Supplier A.....	37
Figure 4.5. The worn cut edge of 2 mm DP600GI specimen from Supplier A.....	37
Figure 4.6. The worn cut edge of 1.1 mm DP600UC specimen from Supplier A.	38
Figure 4.7. The medium cut edge of 1 mm DP600GI specimen from Supplier A.....	39
Figure 4.8. The medium cut edge of 1.5 mm DP600GI specimen from Supplier A.....	39
Figure 4.9. The medium cut edge of 2 mm DP600GI specimen from Supplier A.....	40
Figure 4.10. The medium cut edge of 1.1 mm DP600UC specimen from Supplier A.....	40
Figure 4.11. The fine cut edge of 1 mm DP600GI specimen from Supplier A.....	41
Figure 4.12. The fine cut edge of 1.5 mm DP600GI specimen from Supplier A.....	42
Figure 4.13. The fine cut edge of 2 mm DP600GI specimen from Supplier A.....	42
Figure 4.14. The fine cut edge of 1.1 mm DP600UC specimen from Supplier A.	43
Figure 4.15. The Major strain from ARAMIS just before a large fracture appear. The top edge represents the cut edge. Maximum fracture strain is 0.25.	54

Figure 4.16. The displacement in mm between the simulated geometry of the specimen in AutoForm and the real geometry of the test specimen generated in ARAMIS. This is the displacement value from material no. 5..... 55

Figure 4.17. The major strain value of the sheared cut edge in the simulation in AutoForm at maximum press depth and force before the large fracture appear that will separate the specimen. See diagram 4.13 to see the point in the forming curve. 56

Figure 4.18. The strain at the fracture when maximum force and punch depth is reached just before the fracture grow and separates the specimen. See diagram 4.13 to see the point in the forming curve. ... 56

1 INTRODUCTION

1.1 Introduction

This chapter introduces the background, problem statement and objective of this thesis.

Volvo Cars Body Components (VCBC) in Olofström, Sweden, is Volvo Cars plant for manufacturing of body parts together with development and manufacturing of sheet metal forming dies. Many of the body and steel parts to Volvo cars are stamped and sub-assembled in Olofström and later transported to other Volvo plants around the world for final assembly. Olofström has a long history within the metal forming industry that can be recorded back to year 1735. In 1927 the first body components for Volvo cars were manufactured and in 1969 Volvo Cars bought the plant in Olofström [1].

1.2 Background

Volvo Cars uses different types of Advanced High Strength Steels (AHSS) and one of them is called Dual-Phase (DP) steel. DP steel is used in many of the body parts in Volvo Cars SPA (Scalable Product Architecture) platform due to its great strength to weight ratio. DP steels are also commonly used within modern automotive industry for weight reduction and to increase strength of body parts like beams, cross members and pillars.

Die cutting of DP steels requires different settings compared to die cutting of a conventional low-carbon steel. Volvo Cars struggles today with fractures in the cutting edge, see Figure 1.1, of DP steel parts partly due to wrong settings of the cutting tool or worn tools. The fractures in the shear cut edges appears after the sheet metal forming process is performed in a press.

Another uncertain factor for Volvo Cars is how values of the strains in the cut edge from the forming simulations in FE-program AutoForm compares with real strains in the cut edge when forming parts of DP steel.



Figure 1.1. A fracture in a shear cut edge of a DP steel body part.

1.3 Objectives

The main objective is to develop and test a new punch design that concentrates the strain to the edges of a test specimen. The specimens tested with the new punch will be;

1. Specimens of DP steel from three different suppliers
2. Specimens with various shear cut edge qualities
3. Specimens with various thickness
4. Specimens with two different orientations of the burr zone
5. Specimens with a shear cut edge parallel with lengthwise or transverse rolling direction

The tests will be performed to determine how these factors affect the formability of the specimen's shear cut edges and at what values of the strain fractures appear. Simulations of the punch and specimens in FE-software AutoForm will also be compared with the results from the tests to explore eventual variance in fracture strain for the sheared cut edges [2].

1.4 Delimitations

The tests will be performed with specimens cut out with a shear cutter. Tests could also be performed with specimens cut out with a stamping die. This would give different characteristics to the cut edge compared to a sheared cut edge. Due to no available stamping die for this operation, this type of test will not be included in this research. Future research can be carried out to compare the different cutting methods and how these affect the fraction strain of the edge. More tests could be performed for different thickness of DP steels. This study will focus on steel thickness used by Volvo Cars today.

Similar phenomena with edge fractures could exist in sheet metal forming of aluminum alloys and therefore these materials could also be included in the study. Due to time limitations, this project focuses on DP steels.

1.5 Thesis questions

1. Does the highest strain concentration appear in specimen edges during test using the newly developed punch?
2. How does the quality of the cut edges affect the fracture strain in sheared edges of specimens of DP steel with various types and thickness?
3. Does the rolling direction* or the orientation of burr zone* affect the maximum fracture strain*?
4. Is there a difference in maximum value of fracture strain between simulation in AutoForm and real tests?

* For further explanation of concepts, see chapter 2.

2 THEORETICAL FRAMEWORK

2.1 Dual-Phase (DP) steel

Within the automotive industry most car manufacturers have the ambition to develop as reliable, safe and efficient cars as possible. To be able to manufacture such cars, manufacturers need materials with great strength per weight ratio. DP steels have become an attractive material for body parts that have a major impact to the strength and safety of the car like rails, cross members, pillars, inner bumper reinforcement beams and suspension housing. This is due to the high tensile strength, low yield-to-ultimate strength ratio and relatively low price of the DP steels.

DP steels have a ferrite and martensitic microstructure which gives the material high strength and are classified as Advanced High Strength Steels (AHSS). The hard martensitic phase composes 20%-25% of the microstructure and the rest is composed by the softer and ductile ferrite matrix. The high strength of the DP steel does have a negative impact on the formability compared with low-carbon steels [3]. The tensile strength for DP steels can vary from 500-1000 MPa [4].

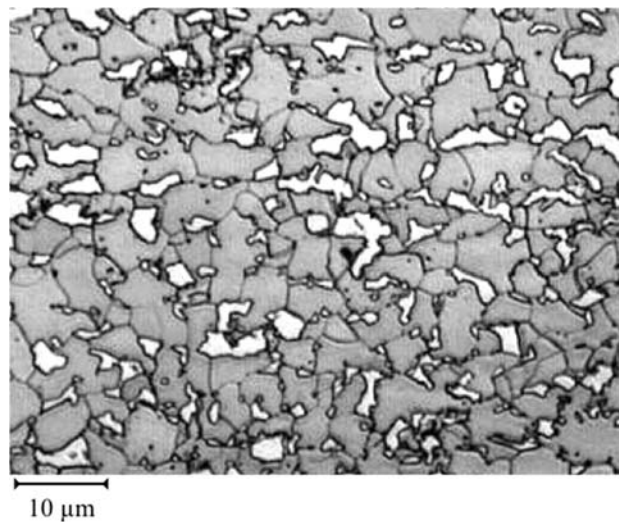


Figure 2.1. The martensitic (white) and ferrite (grey) microstructure of DP steel [5].

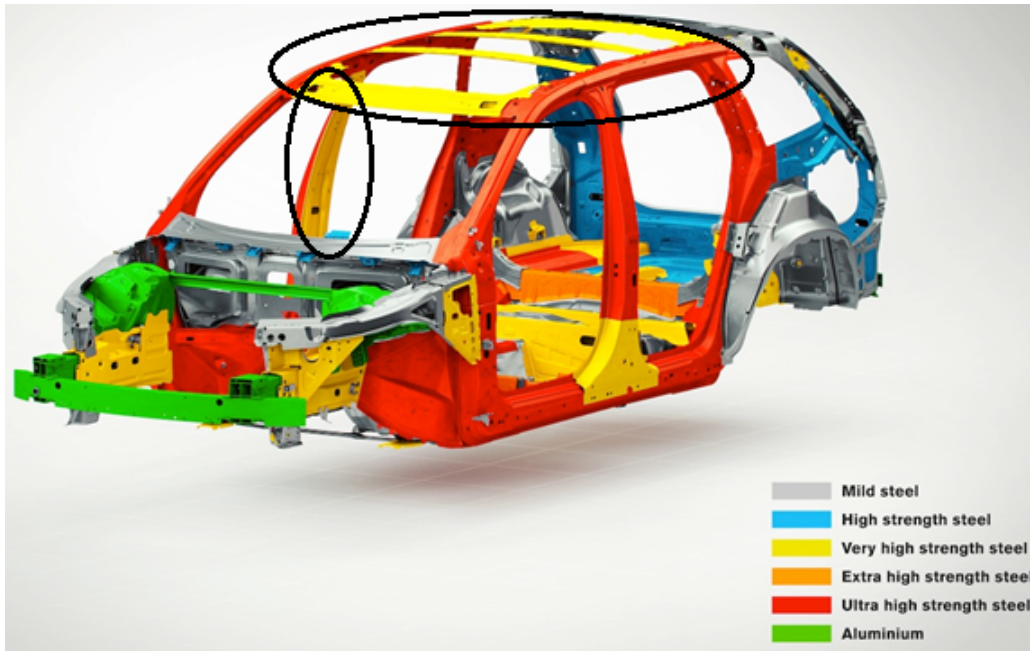


Figure 2.2. The steel body structure of the 2015 Volvo XC90. The marked out parts are examples of parts made of DP steel.

2.2 Shear cutting of metals

The shear cutting procedure can be defined as two edges working towards each other to separate material into smaller pieces. The material between the edges is deformed so that fractures appear and eventually the material will separate. Material properties such as strength, Young's modulus and ductility have great impact on the cutting procedure. When the two edges engage in the material, see Figure 2.4, a fracture will appear on each side and will continue to grow as the edges continue to move through the material.

A basic condition that must be met to perform a shear cutting operation is that the material of the cutting tool needs to have larger hardness and strength than the material to be separated. After a shear cut operation an edge with several different zones appear, see fig. 2.3, and due to different adjustments of the cutting tool the length of this zones can vary. With optimal adjustments of the cut tool the shear zone represents between 25-35 % of the edge surface. For an edge with a big burr zone, the adjustments of the cut tool have not been advantageous.

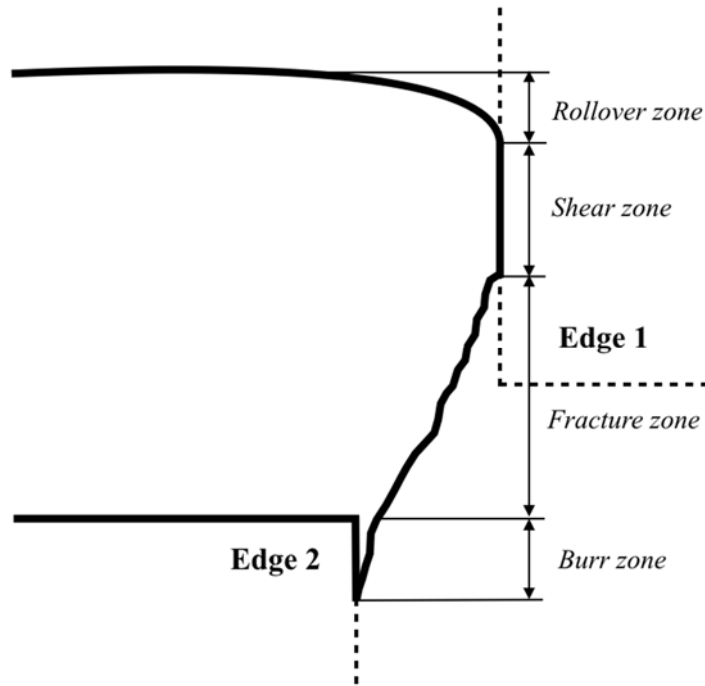


Figure 2.3. The different zones for a shear cut edge.

With optimal adjustments of the shear edges the fractures from each side will meet and thereby separate the material, see Figure 2.4. With increased distance between the edges or with worn tool edges, the fractures won't meet up and thereby more force is acquired to separate the material and the quality of the cut will get worse. Adjustments that can be done to change the shear cut quality is the distance (clearance) between the cut edges, wear of the cutting tool, cutting edge geometry and to add a lubricant. The clearance (d), see Figure 2.5, is a percentage value of the thickness of the material to be cut [6].

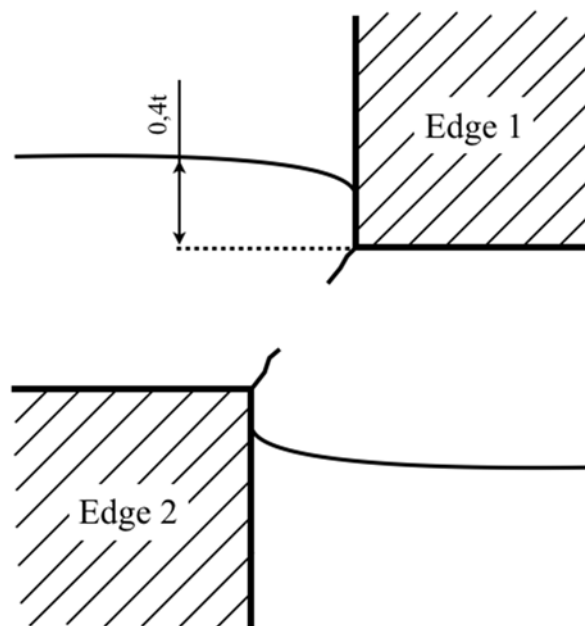


Figure 2.4. With optimal adjustments, the fractures will meet and give a fine cut. When the edge approaches approx. 40% ($0.4t$) of the thickness of the material a fracture will appear.

During the shear cutting operation of the sample, the high tensile load applied leads to extreme deformation to the sample edge. This results in a work hardening of the material around the edge and the formability properties of the material will be changed. This work hardening can lead to edge-fractures during the sheet forming process. The cut edge clearance has a great impact on the work hardening of the edges.

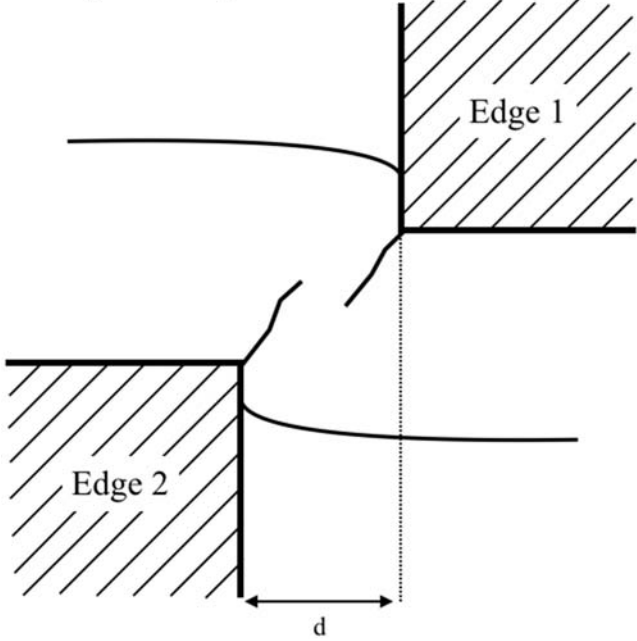


Figure 2.5. With a large clearance between the shear edges, the fractures won't meet up and this will result in worse cut quality.

A clearance of $d = 10\%$ will increase the formability and strain of the sample by 34% compared to a milled edge. With a clearance of $d = 20\%$ the increase on formability and strain is 11% according to [7]. The level of formability of a material is an important factor when performing sheet metal forming.

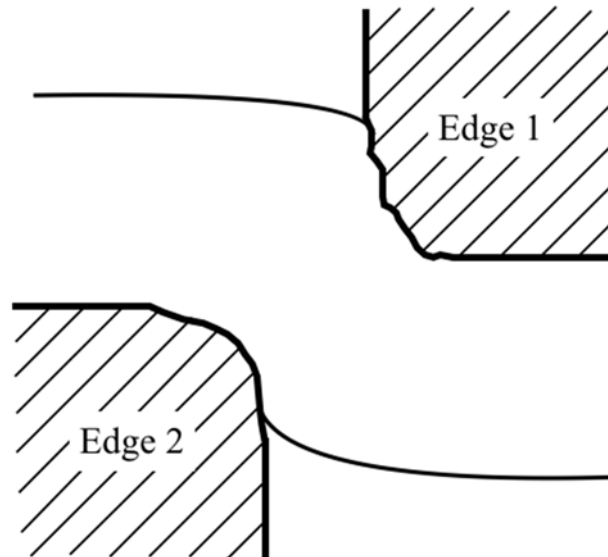


Figure 2.6. Worn edges of the cut tool leads to greater zone of deformation and the fracture will appear later.

2.3 Sheet metal forming

The sheet metal forming process is used to form a metal sheet through plastic deformation, commonly with a die, a punch and a blankholder. The principle is that the metal sheet is held in position between the blankholder and the die while the punch is pressed down towards the die. Therefore, the blank will form after the geometry of the punch and the die. Metal sheets are often formed in a series of forming operations to achieve its final shape. During the sheet metal forming process fractures can appear if maximum fracture strain for the material is exceeded.

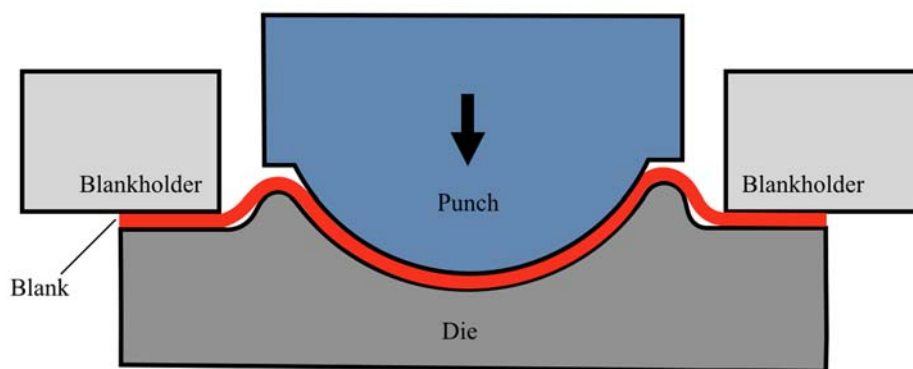


Figure 2.7. Sheet metal forming with the die components.

Another type of sheet metal forming is stretch forming. In this case the blank is locked by applying a high force between the blankholder and die. To form the blank, a punch is pressed against the blank and thereby the blank is subjected to tensile stresses. This will lead to a reduced sheet metal thickness as the punch interacts with the blank [8].

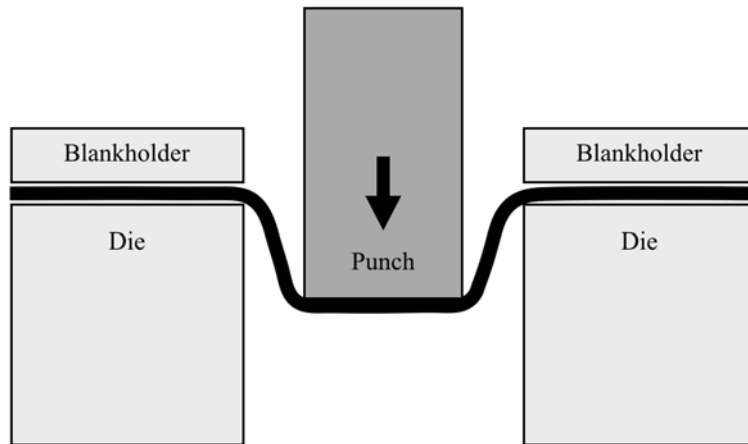


Figure 2.8. Stretch forming.

2.4 Strain

The engineering strain (e) is a dimensionless value of total displacement of particles in a body relative to the initial position. To calculate the strain, the change in length of a specimen (ΔL) is divided by initial length on a specimen (L_i). The engineering strain is used for simple technical calculations with small strains [9].

$$e = \frac{\Delta L}{L_i} \quad (2.1)$$

The true strain (ε) is used for more advanced calculations of the strain and involves changes of the cross-section area (A_i) of the specimen in the equation. The true strain is used for FE-simulations. [10]

$$\varepsilon = \ln \frac{l_1}{l_0} \quad (2.2)$$

and

$$\varepsilon = \ln \frac{A_0}{A_1} \quad (2.3)$$

2.6 AutoForm simulation software

AutoForm is an FE-software developed for the die-making and sheet metal forming industry and is used by many of the largest car manufactures. This software is used to design dies from CAD model of a car part. The sheet metal forming operation can be simulated and strain and stresses can be predicted for different metals. This software is very useful for material, weight and price optimization of sheet metal parts of any kind, see [11] and [2] for more details.

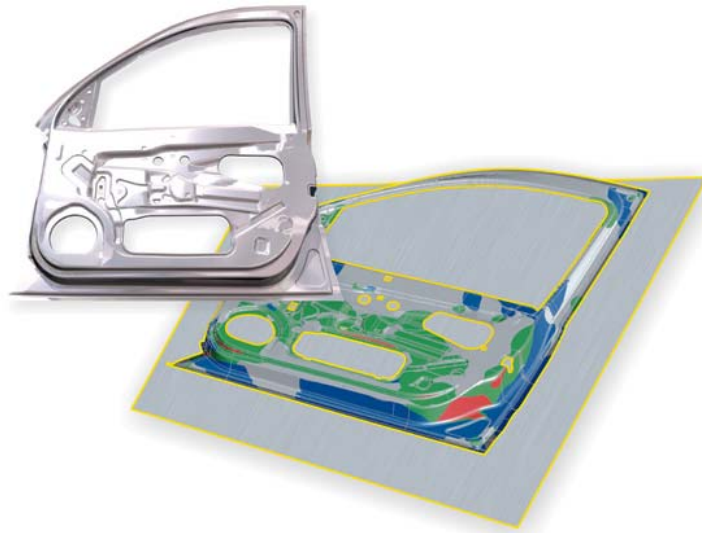


Figure 2.10. FE-simulation in AutoForm.

2.7 ARAMIS measuring system

ARAMIS is a Digital Image Correlation (DIC) system developed to measure displacements, surface strain, velocity and accelerations of a test object. The system creates a 3D measurement resolution and uses digital images to measure changes of the material specimen of just a few millimeters to several meters in size. The measured data is used to determine material properties of the test specimen such as Young's modulus (elastic modulus) and Forming Limit Curves (FLC), see [12] for more details.



Figure 2.11. The two cameras of the ARAMIS system determine changes of the test specimen during a tensile test or similar tests [12].

2.8 Profilometer

A profilometer is a measurement system used to measure surfaces and profiles of details or objects. The system uses a probe or stylus that slides over the surface of an object and a projected picture of the surface will thereby be created from the collected data.



Figure 2.12. The Surfscan measurement system used for measurement of edge geometry in this study.

2.9 Rolling and rolling direction

Rolling can be defined as deformation of a material between two rolls that is rolling in opposite direction, see Figure 2.13. The rolling operation changes and dislocates the crystal structure of the material and thereby the yield strength is increased and the ductility decreased. The lengthwise direction is called the Rolling Direction (RD) and the across direction is called the Transverse Direction (TD). When cutting out specimens from a rolled material to a tensile test, the rolling direction is important to consider due to minor variations in strength and formability in different directions. The formability for a steel specimen with a TD is usually slightly lower than a specimen with RD, see [13] and [14] for more details.

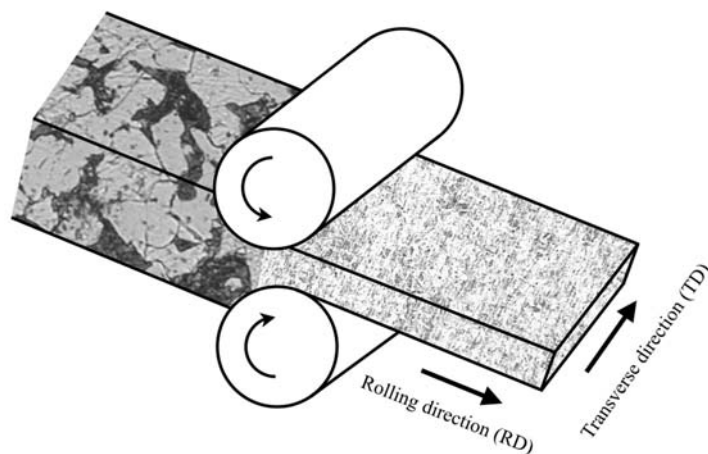


Figure 2.13. The microstructure of the steel changes during the rolling operation.

2.10 Galvanizing of steel

Corrosion and rust of steel can be prevented by galvanization. In this process the clean steel is immersed into molten zinc and thereby a metallurgical reaction between the iron and zinc emerges. This reaction provides the steel with a robust coating on the surface of the steel, preventing oxygen to react causing corrosion. Hot-dip galvanization is one of the most commonly used galvanization methods and the temperature of the liquid zinc bath is usually around 450 °C. The abbreviation for a galvanized steel is GI and for a ungalvanized steel UC (uncoated).

The hot-dip galvanization process has an impact to the material properties of the steel. Earlier research presents a drop of strength for galvanized steel, see [19].

2.11 Related work

E. Atzema and P. Seda has published a paper [16] where they compare different test methods for sheared edge tensile tests to find out how the edge fracture strain varies between the test methods. The different test methods compared is HEC (ISO-16630), KRE (Edge fracture sensitivity test), SET (Sheared Edge Tensile test) and SETi (Sheared Edge Tensile test improved). They claim that the KRE tests method requires too much material for use in a laboratory material development stage. They also explain that the results of the maximum fracture strain from a HEC test scatter considerably and that there is a scope for improvement for this test method. The SET test method is explained as a test method suitable for relatively small test specimens but that the test itself is complicated to execute where one uses the load drop to determine and calculate the fracture strain value. SETi is an improved version of SET where the fracture strain value is determined by using a DIC based strain measurement system. The DIC system uses images to find initial cracks during the tensile test and thereby the fracture strain can be determined much more precisely.

In paper [16] they compare two types of cut shear edges, 10% and 20% cutting clearance, using the SETi test method. They did not find any appreciable microstructural differences between 10% and 20% clearance when they examine the edges with a light microscope and explains that the effect of worn tooling is much larger than extreme clearance. However, they did not investigate how worn cutting tools are affecting the edge quality and the fracture strain of the edge. This thesis aims to examine how worn tooling affect the fracture strain.

In a paper [17] from W. Volk, et al. they describe that the main cause of failure in sheet metal forming simulations are geometric, surface and material defects. They describe that a milled edge sample have approx. 34 % higher formability than a sample with shear cut edges with a die clearance of 10 %. The test method used for this article was the *edge-fracture-tensile-test* developed at the Institute of Metal Forming and Casting in München.

Z.K. Teng and X.M. Chen has published a paper [18] in which they study the edge fracture mechanism of two different DP steels, DP980 and IBF980 (Improved Bending and Flanging). They perform controlled edge tension tests on samples and uses electron microscopy (SEM) to study the result. They explain that the edge fractures are propagated from small pre-existing micro cracks appearing from the initial shearing process. The tests show that IBF980 steel have a higher formability and thereby higher resistance to edge fractures than DP980. The IBF980 steel have a smaller size of the martensite particles that DP980, which has a positive impact on the formability of the material. In this research they did tests in a tensile test machine and this

does not take into account how the formability is affected with the burr zone facing upwards or downwards related to a forming tool.

X. Zhuang, *et al.*, published a paper [19] in October 2014 about failure mode and ductility of cold rolled DP steel DP590. They did tensile tests of dog bone specimens with a thickness of 1.2 mm in the rolling direction. The tensile tests were performed on specimens with four different cut qualities (clearance of the blanking tool). They discovered that overall ductility of the DP steel is dependent on the ductility of the ferrite matrix. They did also determine that pre-existing cracks of the specimen's edges did reduce the overall ductility and changed the failure mode. Just as in paper [16] they used the classic tensile test as a test method and this method does not consider the orientation of the burr zone of sheared edges and how this affects the maximum fracture strain.

Inspiration to the geometry of the punch developed in this study was from a presentation from The International Deep Drawing Research Group 2016 (IDDRG2016) in Linz, Austria, see [20].

3 METHOD

3.1 Project approach

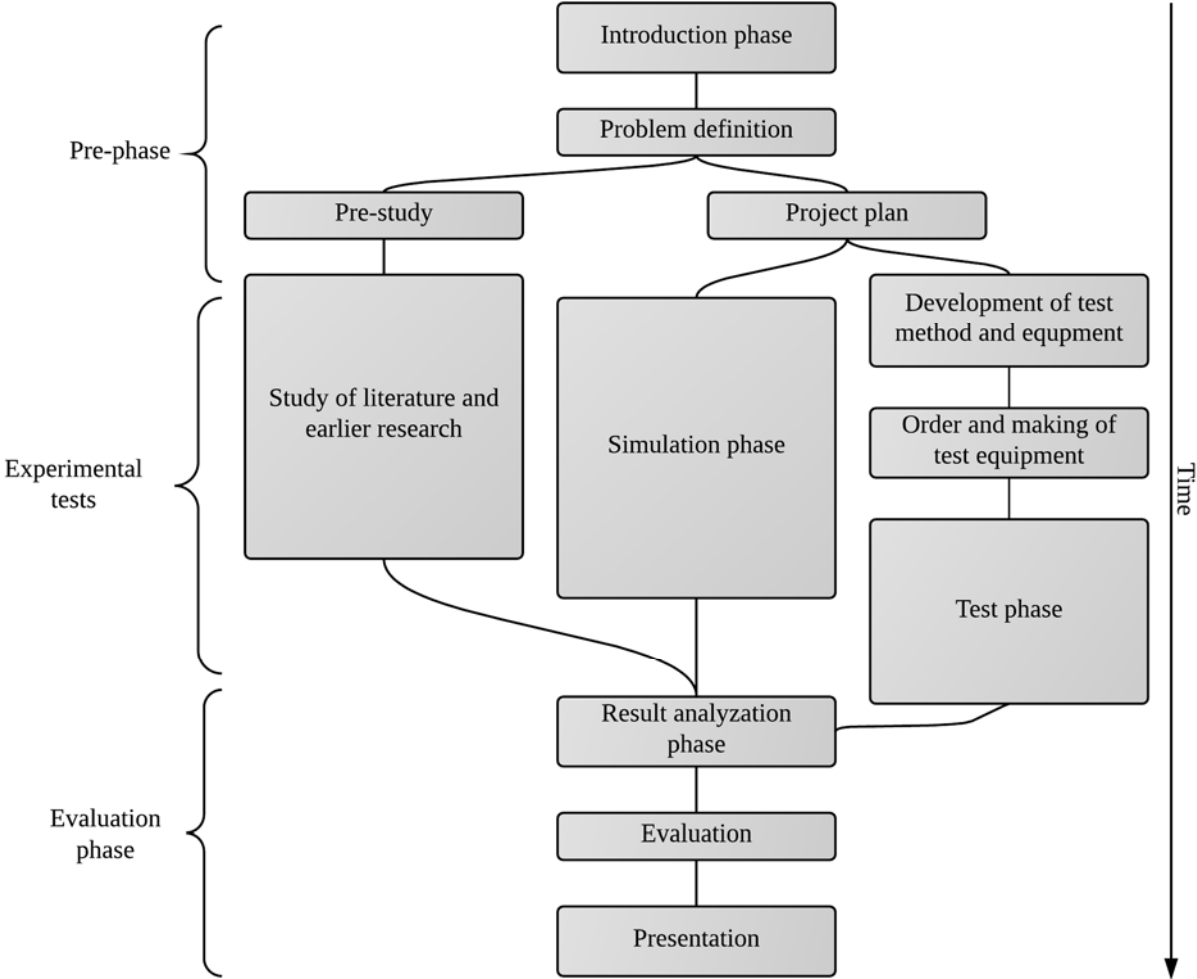


Figure 3.1. A visual schedule over the phases in the current project.

3.2 Study of literature and related research

A study of similar research done about DP steels, test methods and fracture strain was done in the pre-phase of this project. Both literature and papers was read and some earlier research done by Volvo Cars was studied to be sure that the questions of this thesis haven't been answered in earlier reports or papers. Theory used for the theoretical framework of this report was found in relevant literature, papers and from technical experts and personnel at Volvo Cars and Swerea IVF in Olofström, Sweden.

3.3 Tensile tests

All material used in the study, seen in Table 3.1, was first tested in a tensile test machine at three different directions, 0°, 45° and 90° angle to the rolling direction to explore the material behavior of each sheet material used in the study in an early phase. Specimens with the shape of dog bone was used for the tensile tests. Tests was performed on specimens with polished edges and with non-polished edges. The results from the tensile test was used to compare and explore, in an early phase, if the quality of the edge affects the maximum fracture strain of the material.



Figure 3.2. The automatic tensile test machine used for the tensile tests. Dog bone specimens ready for testing can be seen down in the middle.

3.4 Design of the punch geometry

A new punch geometry was developed that was used during the press tests. The idea with the new punch geometry was to create a design that, during tests, concentrates the strain to the edges of a test specimen. Another goal with the new punch was to be able to measure how great impact the orientation of the burr zone of the specimen edge had to the maximum fracture strain. No other official type of punch or test technique is available as a standardized test method for strain concentration at specimen's edges.

The punch was designed in Catia V5 and different geometries was evaluated by simulations in AutoForm. The different geometries of the punch tool were simulated to evaluate which geometry that gave the highest concentration of strain on the edge of the specimen during a press operation.

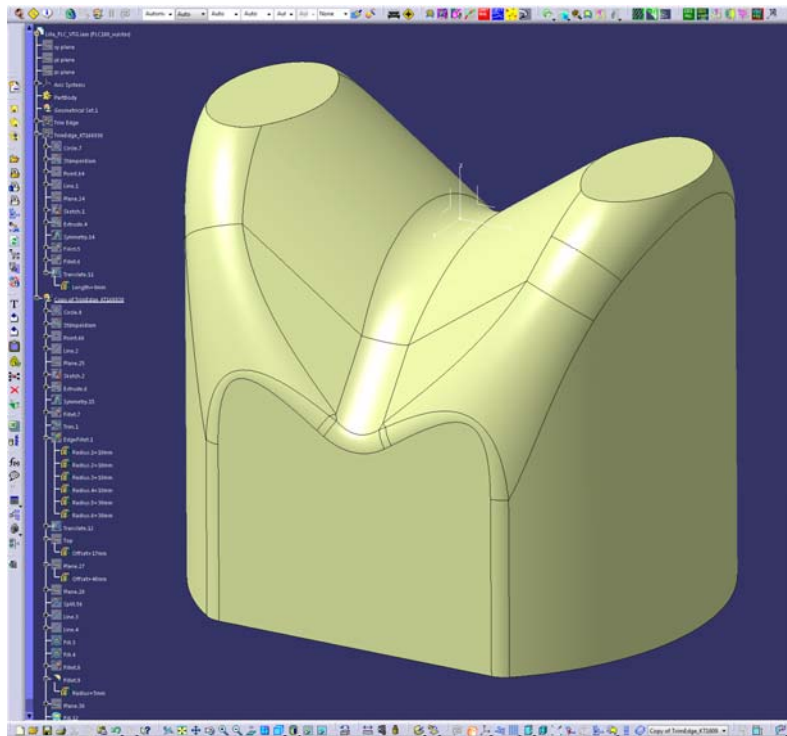


Figure 3.3. Modelling of punch in Catia V5.

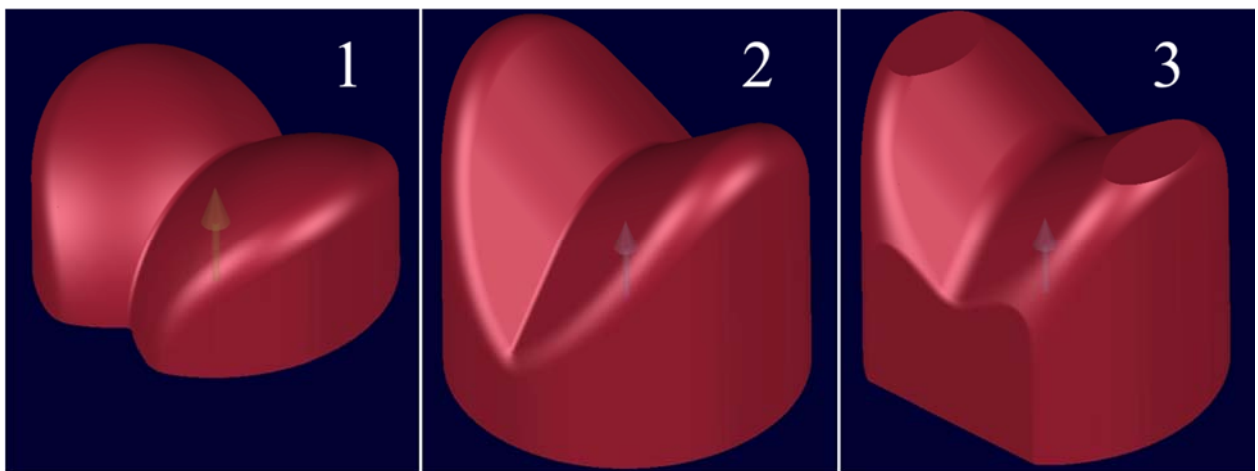


Figure 3.4. The three different geometries of the punch that was created in Catia V5 and analyzed in AutoForm.

For all simulations of the different punch geometry, the same inputs were used to be able to make a fair comparison of the result. After evaluating which geometry that was going to be used, the Catia V5 file was sent to Swerea IVF in Olofström for manufacturing. Catia V5 was used as the CAD program because this is the most commonly used CAD software within the Automotive industry and at Volvo Cars, see [21].

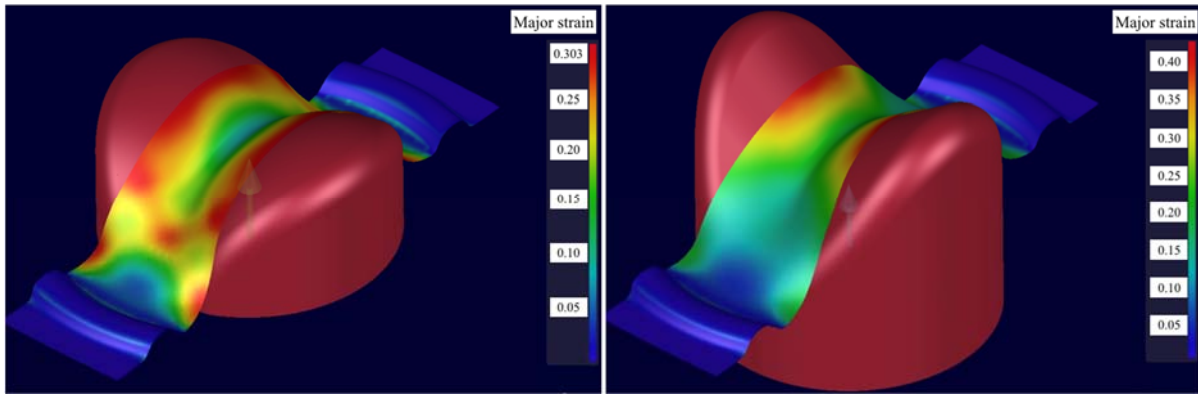


Figure 3.5. The figures present the major strain distribution for the specimen from the simulation using two different designs of the punch.

3.5 Materials tested

Various types of DP steel from different suppliers and thickness was tested in the main tests. Material no. 5, see table 3.3, was used for the pre-tests. The three different suppliers of DP steel are presented in this report as A, B and C.

Material no.	Type	Supplier	Thickness (mm)
1	DP600UC	A	1.1
2	DP600GI	A	1.0
3	DP600GI	B	1.0
4	DP600GI	C	1.0
5	DP600GI	A	1.5
6	DP600GI	B	1.5
7	DP600GI	C	1.5
8	DP600GI	A	2.0
9	DP800GI	B	1.0
10	DP800GI	B	1.5

Table 3.1. The types of DP-steels used in the tests.

The dimensions of all the test specimens were 190 x 50 mm. The reason for this dimension was that it was the optimal dimension for the press die used by Volvo Cars at Swerea IVF for press tests. One of the edges for all specimens tested was polished and this edge of the specimens was used as a reference side representing a perfect edge without any fractures, dents or imperfections.



Figure 3.6. The polished edge of all specimens was prepared in an automatic grinding machine.

The edge on the other side of the specimens was a shear cut edge and three different cut qualities were used for different specimens. These three cut qualities had been selected from the pre-tests explained in Chapter 3.5. Two different cut tools, see Chapter 3.7, was used to cut out specimens with different edges. The clearance between the cut tool and die was changed for the different cut qualities. The two different radius of the cut tools edge is used by Swerea IVF as a standard for a fine and worn shear cut of a steel blank. The three different types of cut edges used were:

Quality no.	Clearance	Cut tool edge radius
Fine	5 %	100-150 μm
Medium	20 %	$\sim 20 \mu\text{m}$
Worn	20 %	100-150 μm

Table 3.2. Three different adjustments of the cut tool were used to cut out the specimens.



Figure 3.7. A test specimen before cut procedure.



Figure 3.8. A finished test specimen after cut procedure.

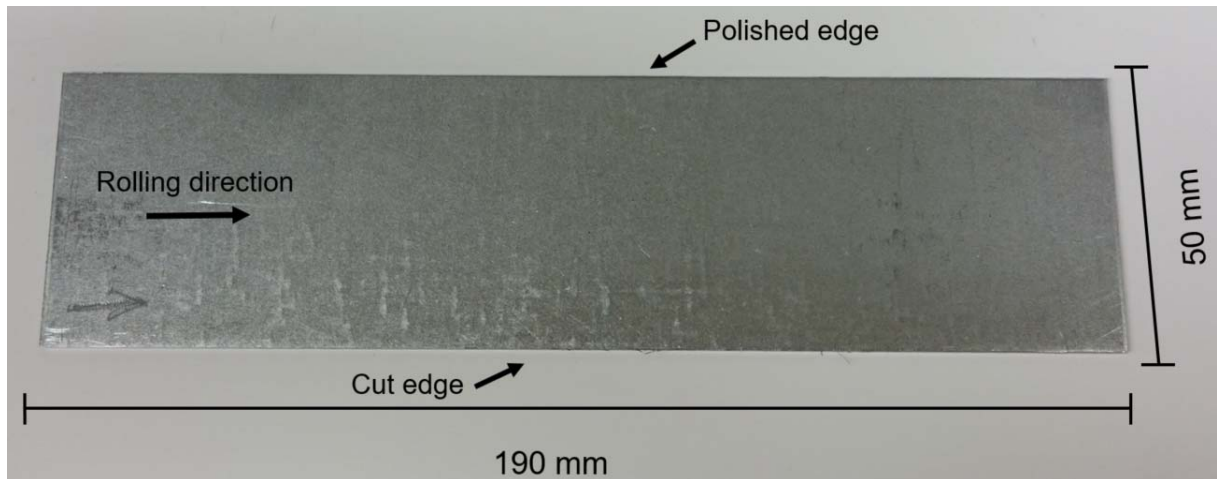


Figure 3.9. A test specimen with one polished and one cut edge. This type of specimen was used during both the pre-test and experimental tests.

3.6 Cut edges of specimens

The different edge qualities were analyzed in a microscope and pictures were taken of the edges. This was done to explore if any fractures could be found in the edges and if there were any differences in the edge zones.

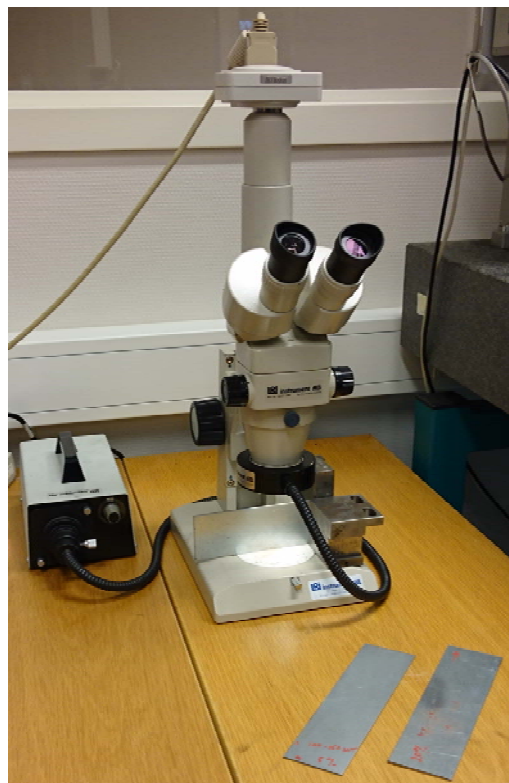


Figure 3.10. The microscope used to analyze the cut quality of the edges.

3.7 Radius measurement of cutting tool edges

Two different cutting tools were used to cut out the test specimens.

Tool no.	Type	Edge radius
1	Fine	~ 20 μm
2	Worn	100-150 μm

Table 3.3. Two types of cutting tools were used.

The geometry of the edges was measured before and after the cut operations of the test specimens using a profilometer (Surfascan surface measurement system). The system uses a probe to measure the geometry of the edge and projects the surface as a picture that can be used for measurement and analyzation. The measurements were performed before and after the cutting operation to explore eventual wear or changes in the edge geometry. The radius of cutting tool edges was measured on five different positions of the edge and the average value of the radius was calculated.

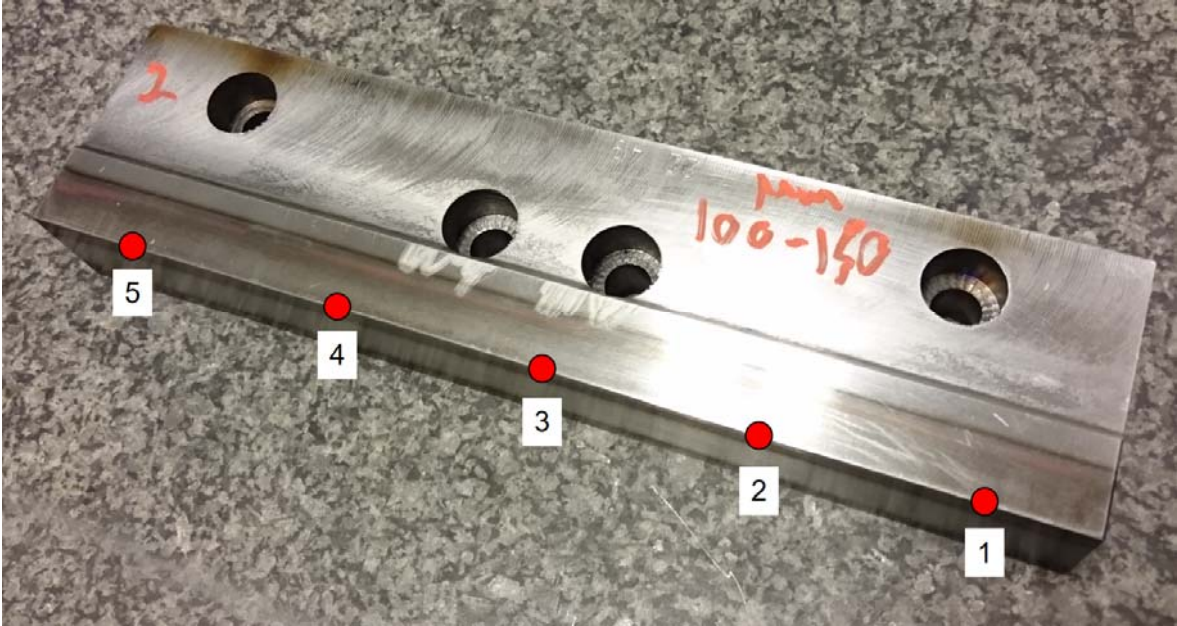


Figure 3.11. The edge radius was measured in five different positions of the tool edge.



Figure 3.12. The Surfscan probe during measurement of worn cut tool.

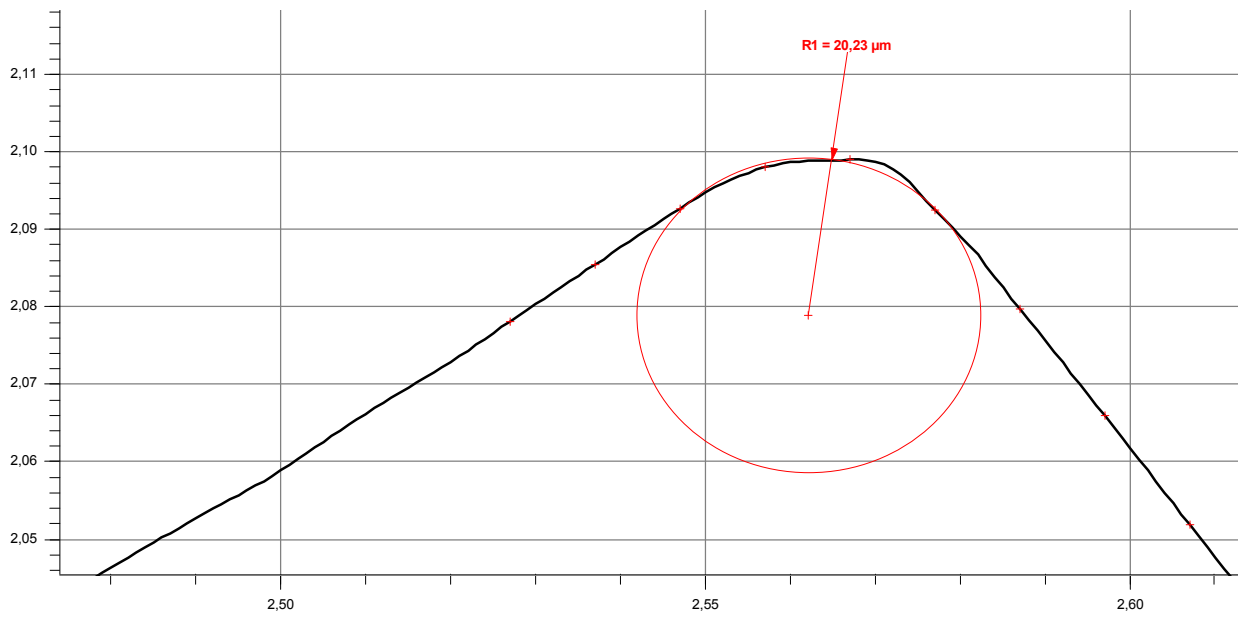


Figure 3.13. A projection of the fine edge from the Surfscan measuring program.

3.8 Pre-tests

The objective with the pre-test phase was to test the CTEST punch with several test specimens to set optimal settings to achieve desired result from the press operation. Another objective was to determine three types of cut qualities (worn, medium and fine) to use for the test specimens for the main tests. The reason to choose these three types was that three different adjustments of cut qualities can be defined for a blank in AutoForm. Thereby the results from the main tests can be compared and transferred to the simulations in AutoForm.

The punch was installed in the press and test specimens were prepared. The test specimens were painted with a stochastic pattern, enabling the ARAMIS measuring system to perform measurements of the strain during the press operation. One painted specimen was placed in the press and formed until the tensile strain was exceeded. Sensors were used during the forming process to measure the punch force and the punch displacement in the press and the ARAMIS cameras filmed the process to be able to measure the strain. All pre-tests were performed with DP steel from Supplier A with a thickness of 1.5 mm and various cut qualities of the edges.

The press operations were performed both with and without oil and Teflon to explore how it affected the friction and thereby the result. Tests were performed with the burr zone of the specimen facing both upwards and downwards (related to the punch) to explore eventual differences of the formability and maximum fracture strain. Totally seven different test with all different parameters and adjustments possible were performed and this is presented in Table 3.4.



Figure 3.14. Installation of the CTEST punch in the press.



Figure 3.15. The painted test specimen was placed in the press and later formed until the maximum tensile strain was exceeded. The same test method was used for the experimental tests.

Test no.	Oil	Teflon	Burr zone	Edges
1	No	No	Up	One cut and one polished
2	Yes	Yes	Up	One cut and one polished
3	Yes	Almost whole area	Up	One cut and one polished
4	Yes	Yes	-	Both polished
5	Yes	Yes	Down	One cut and one polished
6	Yes	Almost whole area	Up	One cut and one polished
7	Yes	Yes	Down	One cut and one polished

Table 3.4. This table shows the different types of specimens and adjustments tested in the pre-test phase.

3.9 Experimental tests

These tests were performed in the same way as the pre-tests but with the exact same adjustments for all material tested. Material no. 5, see table 3.5, was tested during the pre-tests. Material no. 1-4 and 6-10, see Table 3.5, were tested in the second run of tests with the burr zone facing upwards. The rolling direction of all the test specimens was lengthways (RD). Totally 97 tests were performed in this phase. The reason for these adjustments of the rolling direction and burr zone can be found in the results in chapter 4.6 and 4.7.

Test no.	Material no.	Supplier	Thickness (mm)	Type
1	5	A	1.5	DP600GI
2	2	A	1.0	DP600GI
3	3	B	1.0	DP600GI
4	4	C	1.0	DP600GI
5	1	A	1.1	DP600UC
6	6	B	1.5	DP600GI
7	7	C	1.5	DP600GI
8	9	B	1.0	DP800GI
9	10	B	1.5	DP800GI
10	8	A	2.0	DP600GI

Table 3.5. This table presents the order of all tests performed in the press.



Figure 3.16. A specimen before the press operation.

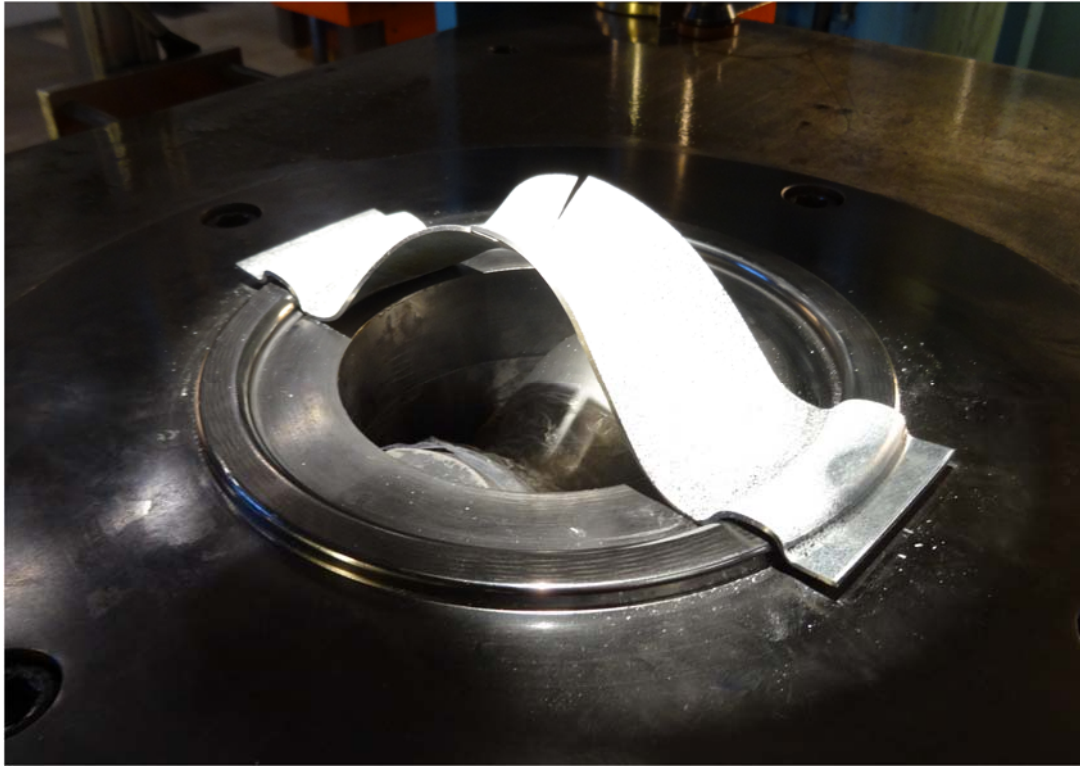


Figure 3.17. A specimen after the press operation. The fracture can be seen at the top of the specimen.

The punch force and the punch depth were measured with sensors in the press. The ARAMIS DIC system filmed all press procedures of specimens. At least two specimens of each type were tested to be sure to not have any unpredictable differences between the results within the same material. If severe differences of the results occurred, one or more specimens of the same material were tested.



Figure 3.18. The press used for all tests. The two computers used for measuring can be seen in front of the press. One computer was used to measure forces and punch depth and the other computer was used for the ARAMIS DIC system.

3.10 Comparison and evaluation of results

3.10.1 Compilation of results in Excel

All data from the force vs. punch depth measurements were compiled in an Excel document and diagrams were created for each specimen type. All tests performed in the press were also simulated in AutoForm. Data of forces and punch depth from the simulations could be put in and compared in the same diagram as the press results.

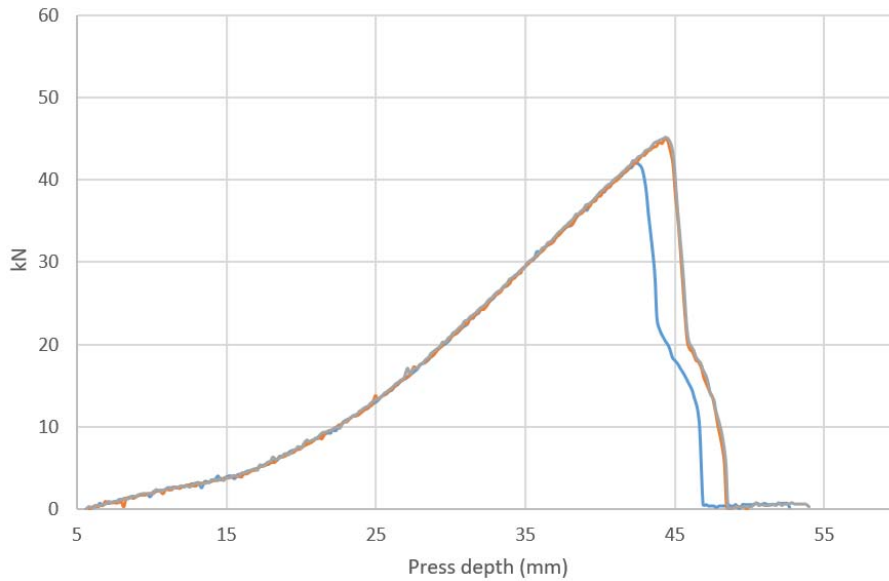


Diagram 3.1. The type of force/punch depth diagram used for comparison of result between simulation and real test. All results were also presented using this type of diagram.

3.10.2 Simulation in AutoForm

The punch designed in Catia V5 were imported as the punch and the test specimen were imported as the blank. The rolling direction (roll angle) were set to RD (0°). Totally 30 different simulations were done, one for each type of material type and cut quality (10 * 3 = 30) tested in the main test phase presented in Table 3.5.

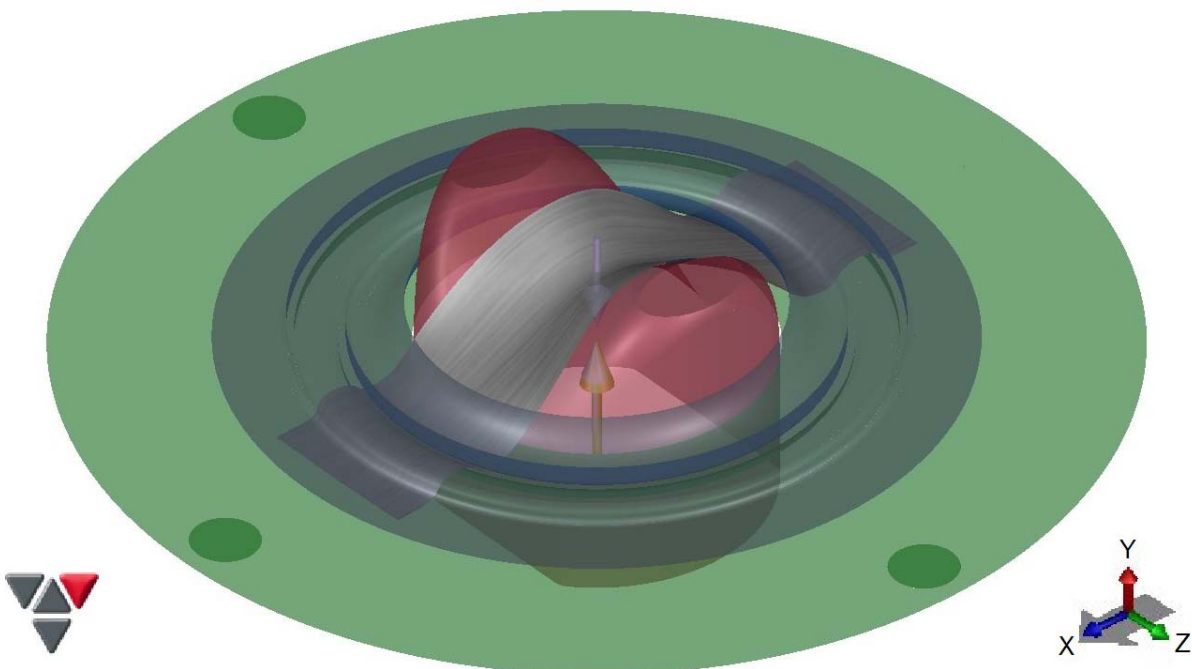


Figure 3.20. An overview of the die, binder, punch and specimen used for the simulation. The same type of tools was used during the physical press tests.

The simulation in AutoForm were performed in the following steps:

1. Maximum punch depth (where the specimen did break) from the main tests were adjusted to be the same in the simulation. This is done by adjusting the gap at bottom for the defined punch.

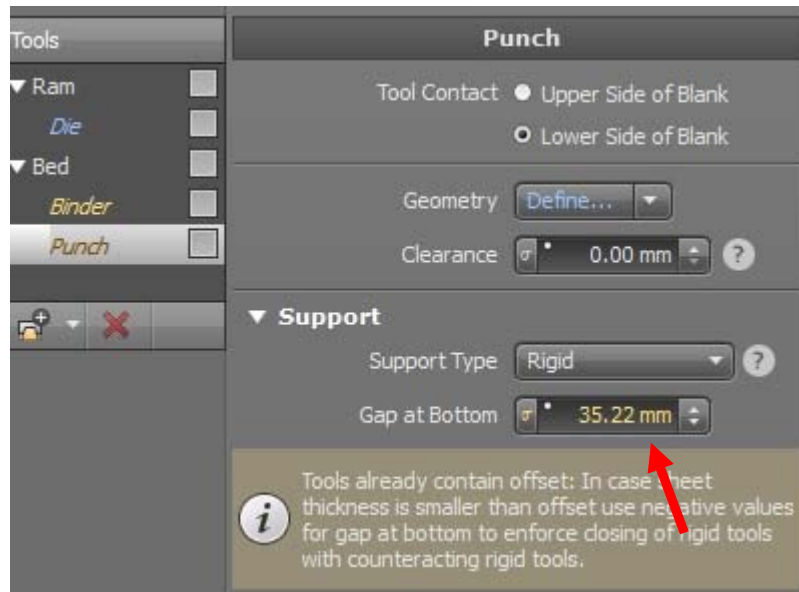


Figure 3.21. The gap at bottom was adjusted for each specimen type to the same distance as where the real test specimen did break from the main tests.

2. Material data from Volvo Cars database were recorded.

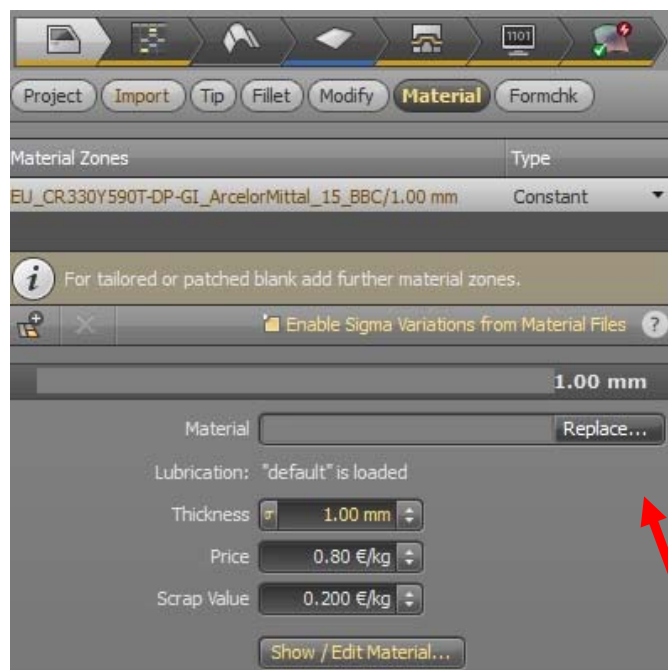


Figure 3.22. Material data for each supplier and type of steel was changed for every new type of specimen simulated.

3. Maximum edge strain were adjusted for each edge cut quality. Then the calculation was started.

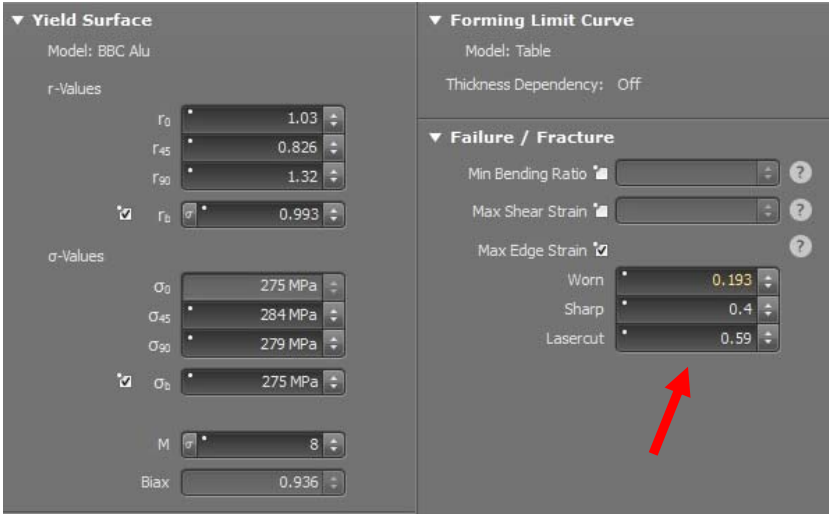


Figure 3.23. The maximum edge strain was edited and adjusted for each specimen tested to get the edge crack value as close to 1 as possible.

4. Evaluation of result and risk of edge crack.

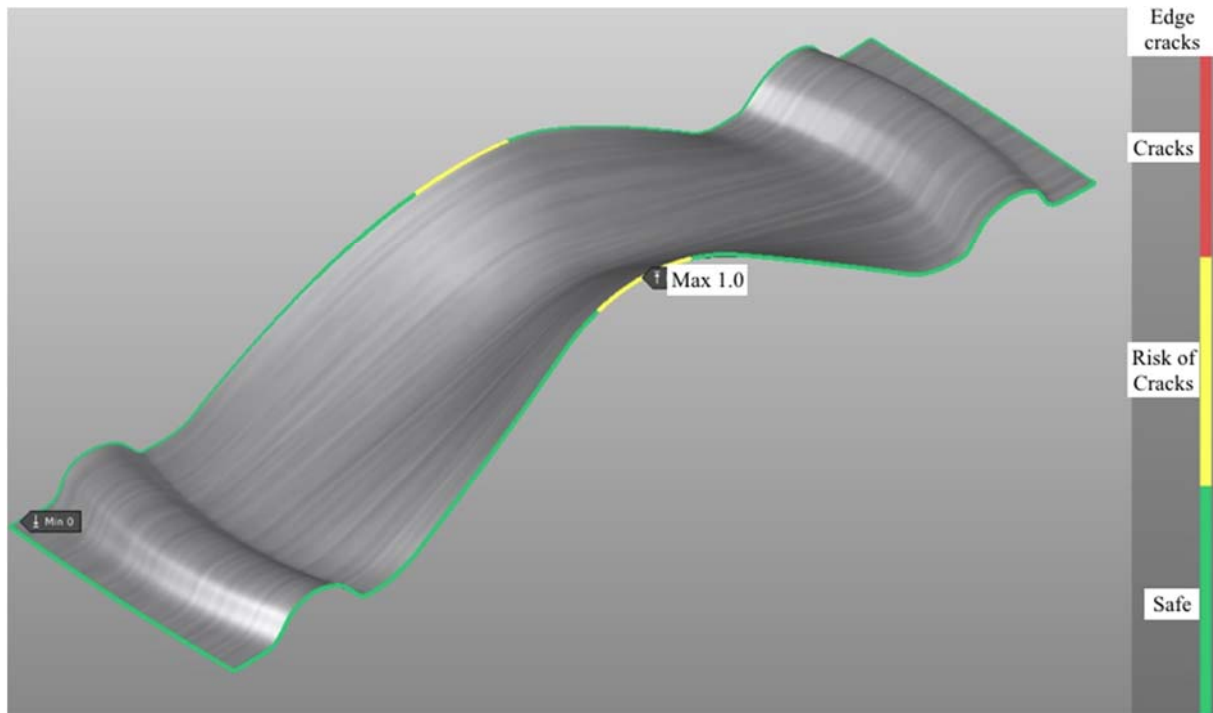


Figure 3.24. The “edge crack” function in AutoForm presents where on the specimen there is a risk for fractures and thereby where the highest strain can be found. All values over 1 means that a fracture will appear.

The function, risk of edge crack, was used to set and adjust the edge strain values. The edge crack value needs to be as close to 1 as possible. If the risk of crack value exceeded 1, the values of the edge strain were adjusted to an optimal value. These simulations were done for all 30 different simulations to adjust the edge strain value and material data to coincide with the real test results.

The friction value in AutoForm was set to different values to test which value that gave similar results as the real press tests. This was done by exporting data from the forces and punch depth and comparing this data with results from the real press tests in a diagram.

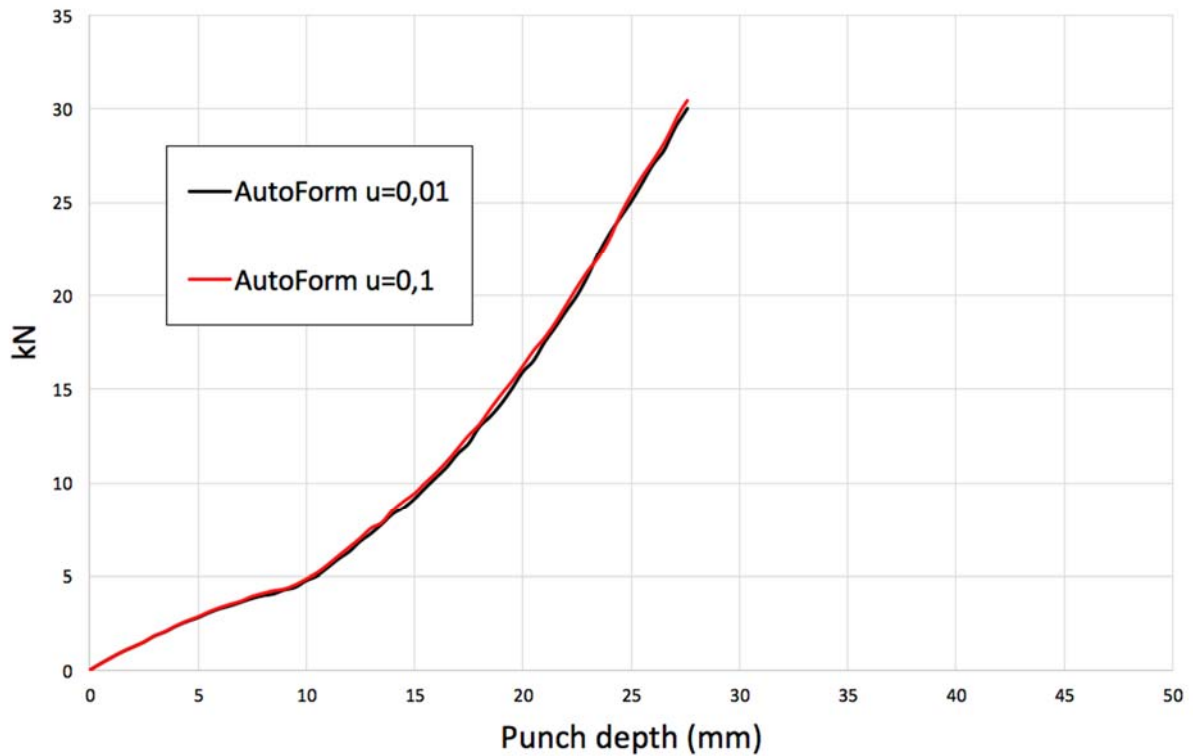


Diagram 3.2. Different values of the friction coefficient were compared to determine how the friction affected the result from the simulated press operation in AutoForm.

For all simulations, the friction value or coefficient was set to $\mu = 0.1$.

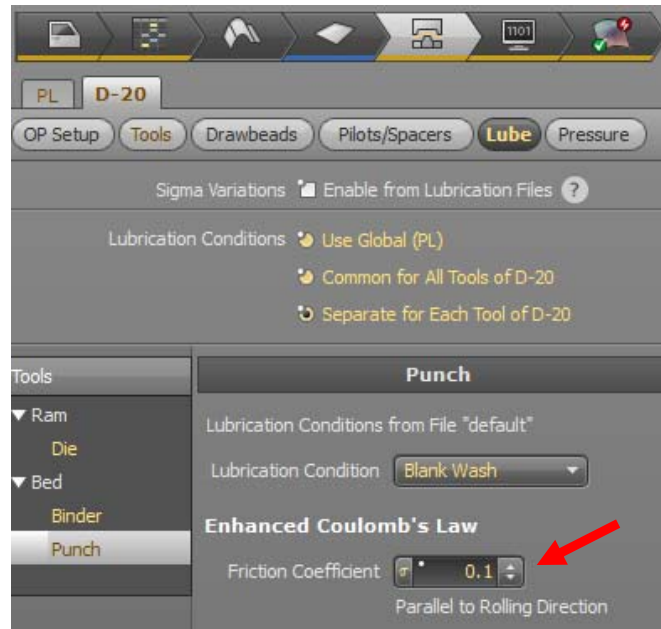


Figure 3.25. The friction coefficient was set to 0.1 for the simulation in AutoForm.

3.10.3 Evaluation of press experiments in ARAMIS

The filmed press tests were analyzed in ARAMIS. The major strain of the specimen and the punch force vs. punch depth curve was analyzed and evaluated. ARAMIS was also used to analyze the behavior and characteristics of the different cut edge qualities to determine when fractures appear during the press test.

3.10.4 Comparison of geometry of simulation and ARAMIS

The geometry of the specimen from the simulation in AutoForm was compared to the geometry of the real test specimen. The geometry of the real test specimen was generated in ARAMIS. The geometry from the simulation in AutoForm was exported into ARAMIS where the geometries could be compared against each other. The reason to do this comparison was to make sure that the geometry of the test specimen was similar between the simulation and the real press test. Eventual displacements between the simulated and real specimen was measured in ARAMIS.

4 RESULTS

4.1 Tensile tests

Both the trimmed and polished specimen endured similar maximum values of stress. The specimen with trimmed edges has a slightly lower value of fracture strain than the polished specimen. A similar relationship between the two types of dog-bone specimens was seen for all material tested. Diagram 4.1 shows that the quality of the edge does affect the fracture strain of the material.

The surface of the polished edge is even and has no imperfections or dents. The trimmed edge looks like a cut edge seen in Figure 2.3 and this edge contains imperfections. These imperfections on the trimmed edge is the reason to that the formability is lower than for the polished edge.

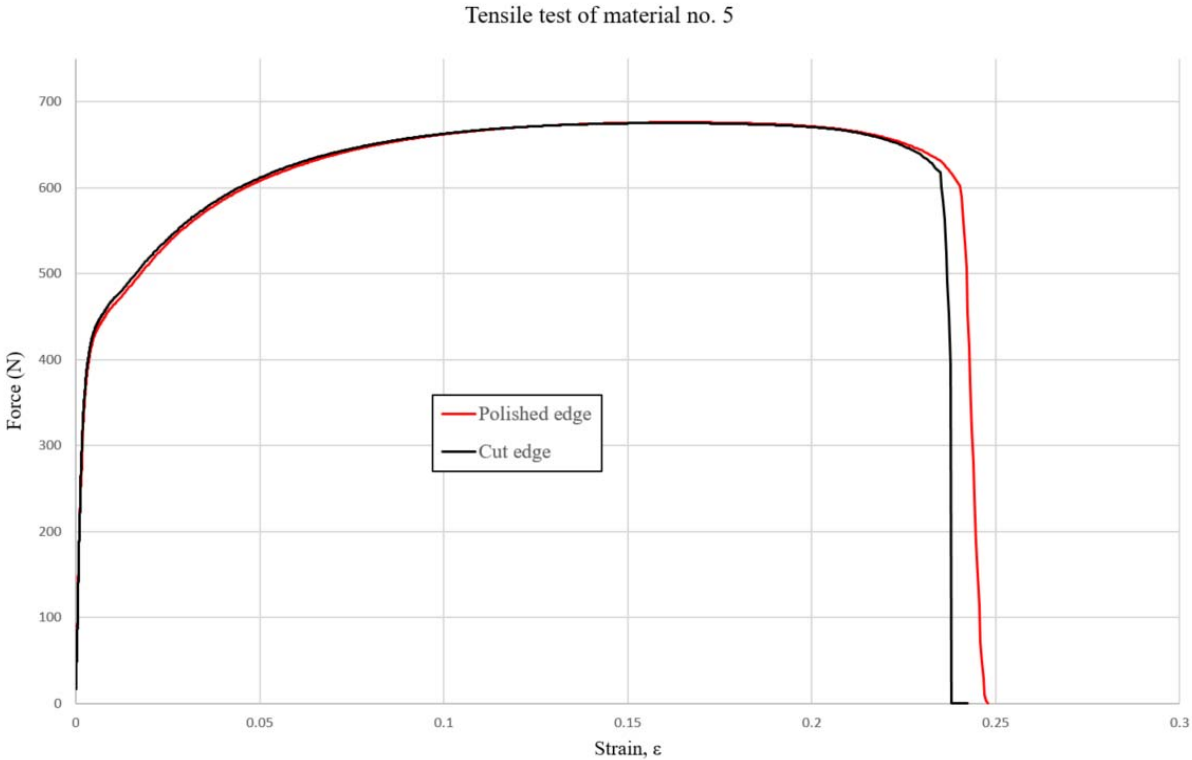


Diagram 4.1. The engineering force-strain diagram from the tensile test of material no.5 (1.5 mm DP600GI from Supplier A).

4.2 Design of the punch geometry

The design of the punch shown in Figure 4.1 was the one used in all tests since it had the optimal geometry for maximum concentration of the strain on the edge of the specimen. This test method is hereby called *CTEST* (Concentrated Trim Edge Strain Test).



Figure 4.1. The CTEST punch.

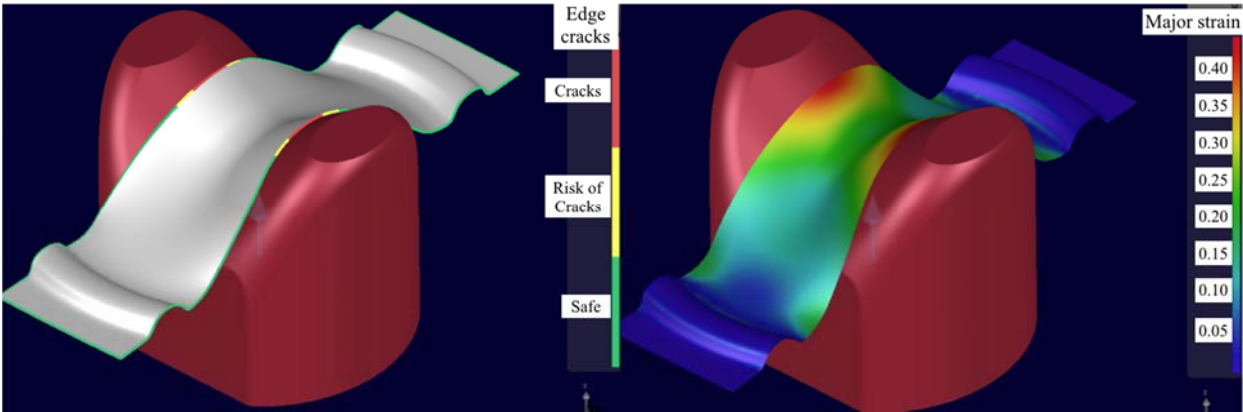


Figure 4.2. FE-simulation of the final design of punch. The left picture presents the risk of edge crack and the right picture presents the major strain.

4.3 Cut edges of specimens

Figure 4.3-4.14 presents pictures of the three different cut qualities of the test specimens from Supplier A with all different thickness used in the tests. A more detailed description of the three different cut qualities used is presented in chapter 4.5.

4.3.1 Worn cut - worn tool and 20 % clearance

The exact same adjustments of the shear cut tool have been used for Figure 4.3-4.6. The clearance was changed depending on the material thickness.

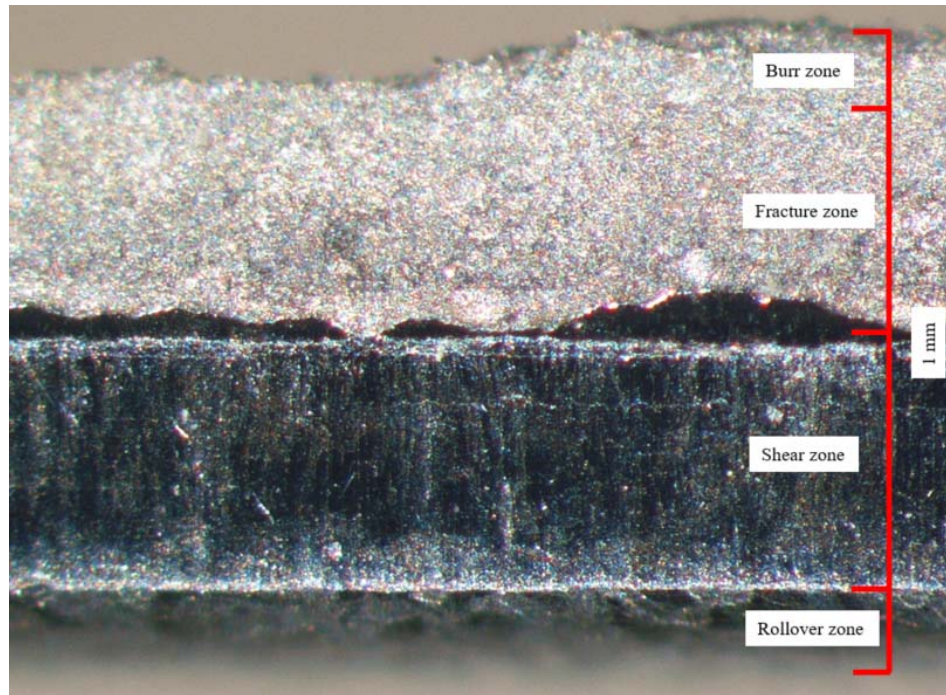


Figure 4.3. The worn cut edge of 1 mm DP600GI specimen from Supplier A.

Figure 4.3 show the worn cut of the 1 mm DP600GI specimen from Supplier A. The shear zone constitutes of more than 50 % of the edge surface. The burr zone is big and very uneven.

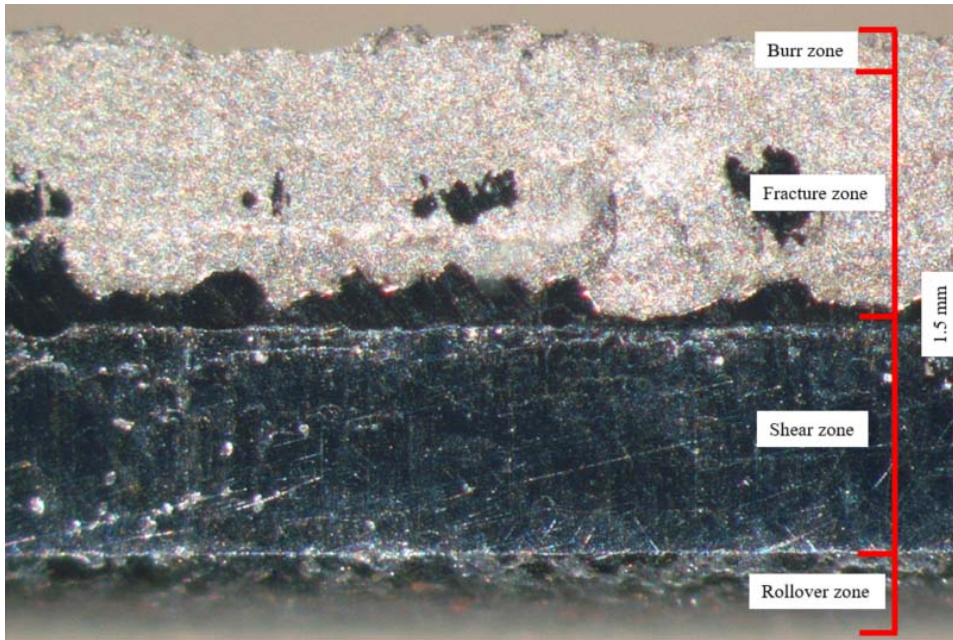


Figure 4.4. The worn cut edge of 1.5 mm DP600GI specimen from Supplier A.

Figure 4.4 shows the worn cut for the 1.5 mm DP600GI specimen from Supplier A with the worst cut adjustments used in the tests. For this quality, the shear zone and the fracture zone constitute of almost 45-50 % of the edge surface. The burr zone is big and small fractures and imperfections can be found in this zone.

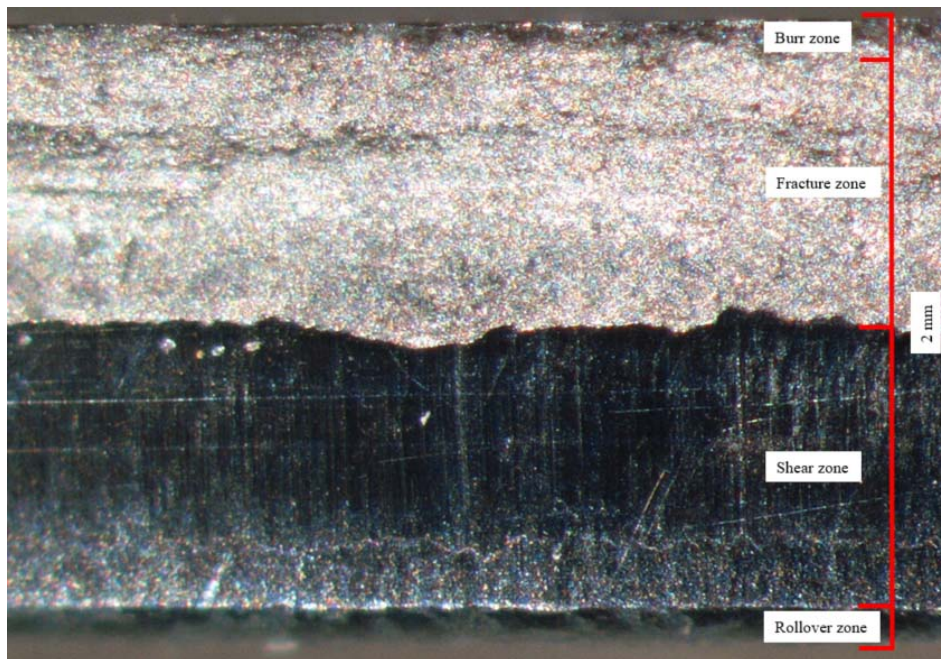


Figure 4.5. The worn cut edge of 2 mm DP600GI specimen from Supplier A.

Figure 4.5 presents that the edge surface of the worn cut of the 2 mm DP600GI specimen from Supplier A constitute approx. 50 % of the fracture zone and the shear zone. The burr zone is large relative the thickness of the material. The burr zone is also uneven and small micro cracks exists in the burr zone.

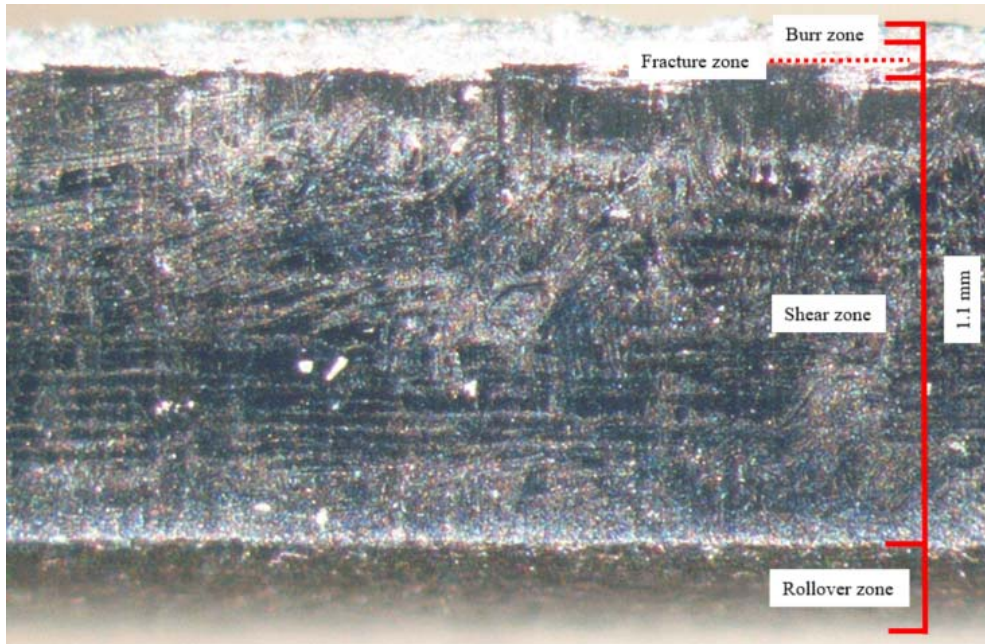


Figure 4.6. The worn cut edge of 1.1 mm DP600UC specimen from Supplier A.

Figure 4.6 presents a very bad cut for the 1.1 mm DP600UC specimen from Supplier A and almost all the edge surface consists of the shear zone. The fracture zone barely exists and the burr zone is uneven.

4.3.2 Medium cut - fine tool and 20 % clearance

The exact same adjustents of the shear cut tool have been used for Figure 4.7-4.10. The clearance was changed depending on the material thickness.

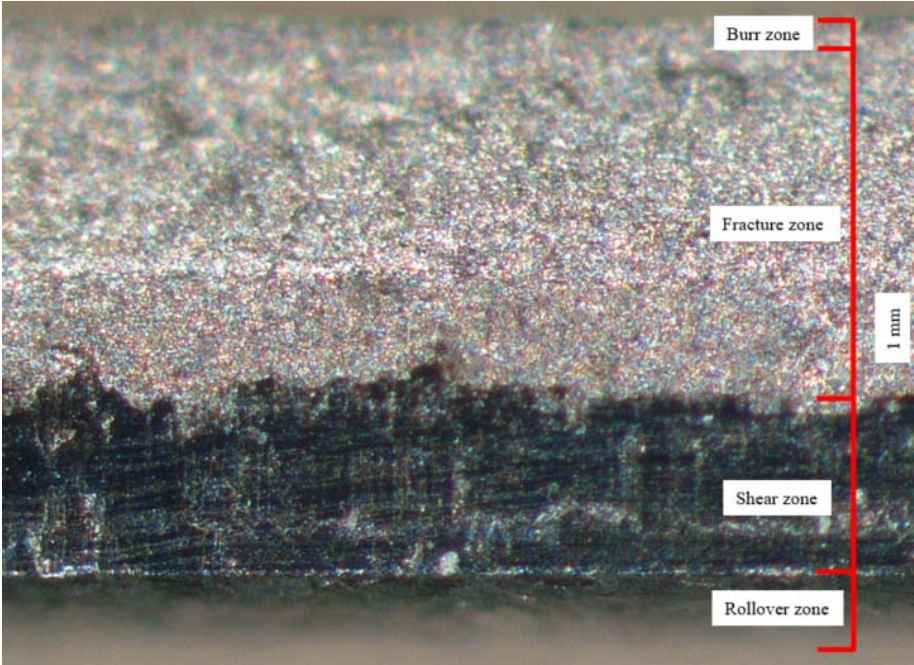


Figure 4.7. The medium cut edge of 1 mm DP600GI specimen from Supplier A.

Figure 4.7 shows the medium cut of the 1 mm DP600GI specimen from Supplier A. The shear zone is representing 25 % of the cut edge surface. The transition between the shear and fracture zone is relatively uneven. A small burr zone exists in this edge.

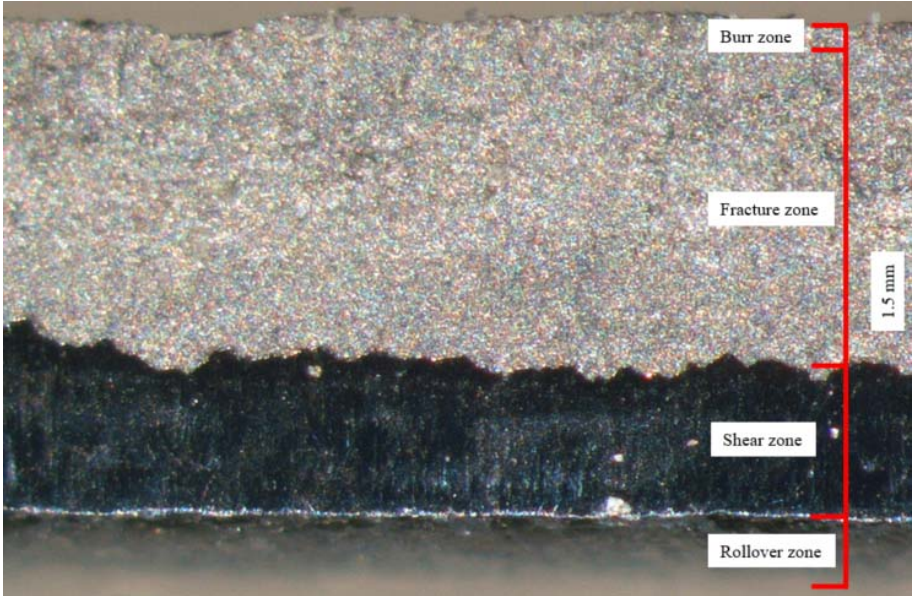


Figure 4.8. The medium cut edge of 1.5 mm DP600GI specimen from Supplier A.

For the medium cut quality of the 1.5 mm DP600GI specimen from Supplier A seen in Figure 4.8, the shear zone represents approx. 30 % of the edge surface and the fracture zone represents 65 %. The burr zone are small and the top of the burr zone are more even than for the worn cut edge.

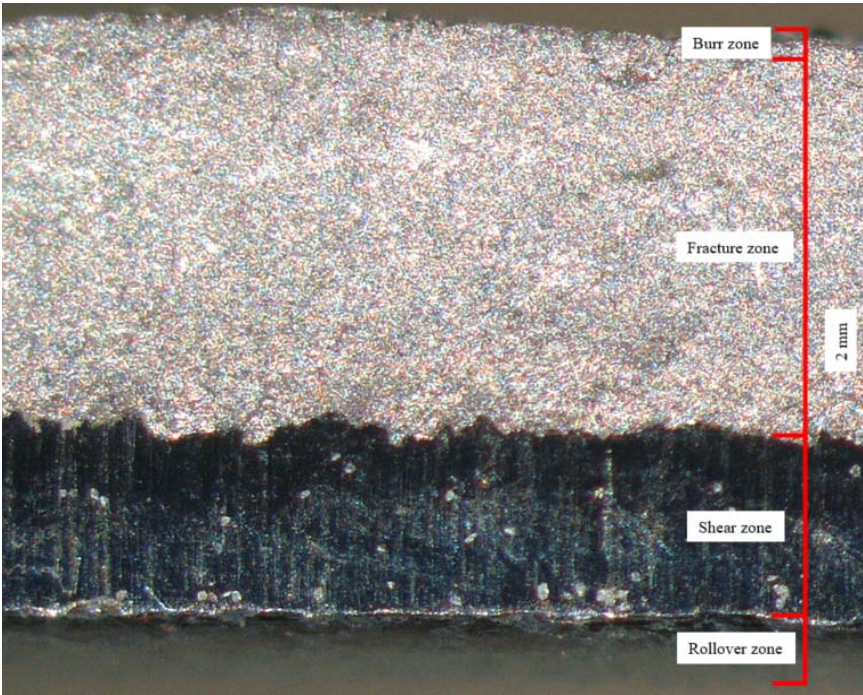


Figure 4.9. The medium cut edge of 2 mm DP600GI specimen from Supplier A.

The shear zone of the medium cut 2 mm DP600GI specimen from Supplier A, represents 30 % of the edge and a small burr zone exists in the edge presented in Figure 4.9. The burr zone is small relative the thickness of the material.

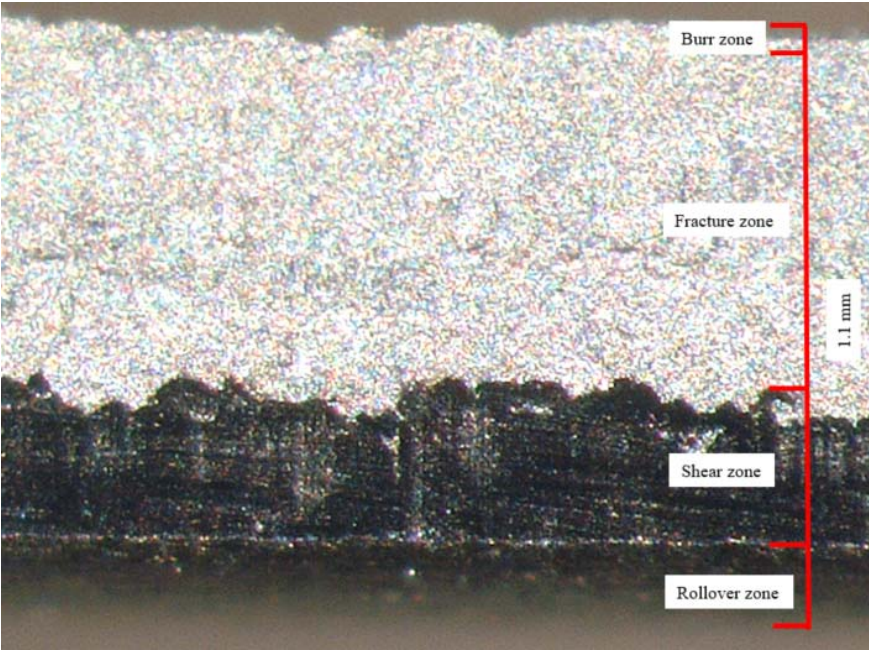


Figure 4.10. The medium cut edge of 1.1 mm DP600UC specimen from Supplier A.

Figure 4.10 presents the medium cut edge of the 1.1 mm DP600UC specimen from Supplier A and this is a great example of a medium cut quality edge. The shear zone represents 30 % of the edge and a small burr zone exists. Small dents and scratches can be seen at the surface of the shear zone.

4.3.3 Fine cut - worn tool and 5 % clearance

The exact same adjustents of the shear cut tool have been used for figure 4.11-4.14. The clearance was changed depending on the material thickness.

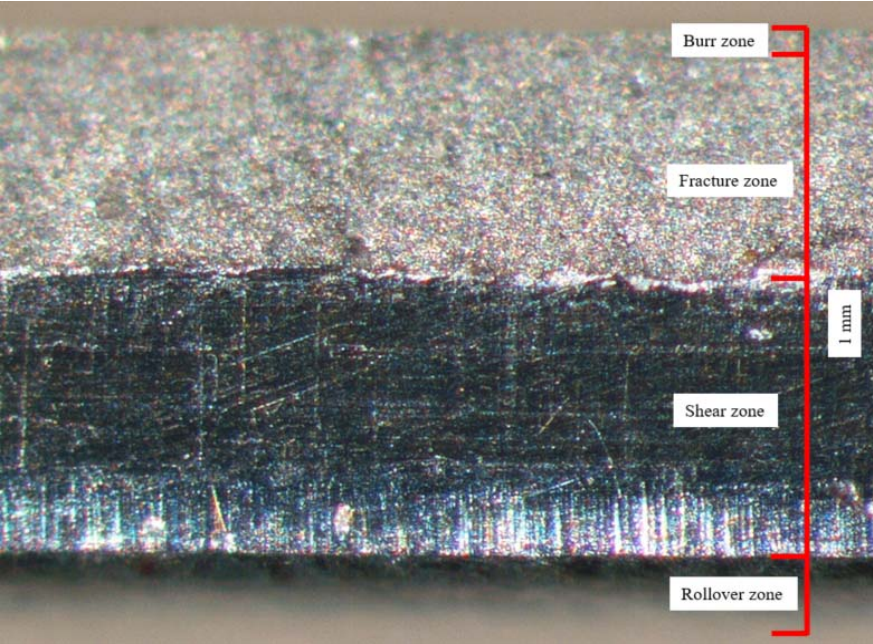


Figure 4.11. The fine cut edge of 1 mm DP600GI specimen from Supplier A.

The shear zone for the fine cut edge of the 1 mm DP600GI specimen from Supplier A presented in Figure 4.11 does represent a to big part of the surface. The adjustments for the fine cut have not been optimal for 1 mm steel specimen.

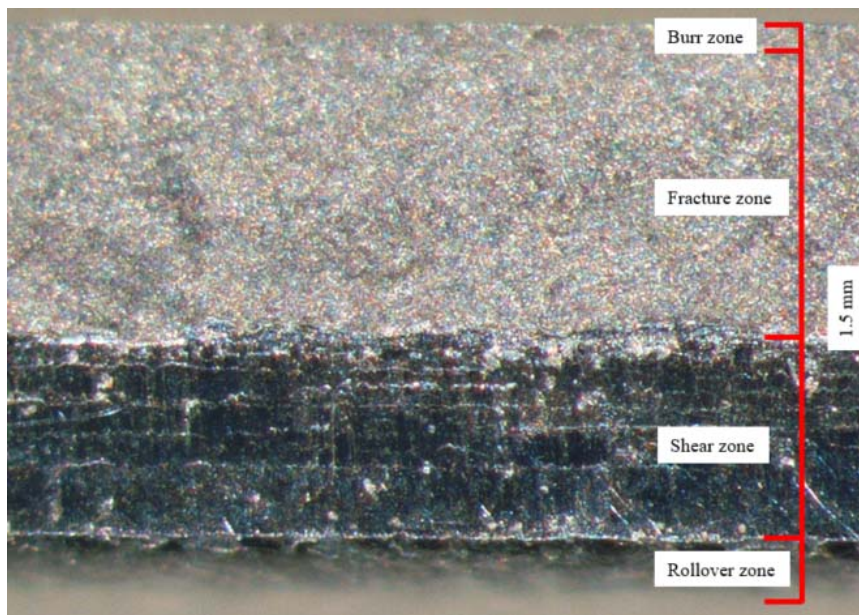


Figure 4.12. The fine cut edge of 1.5 mm DP600GI specimen from Supplier A.

The fine cut for the 1.5 mm DP600GI specimen from Supplier A seen in Figure 4.12, have almost no burr zone and the line between the shear zone and fracture zone are very even and fine. The shear zone represents approximately 35-40 % of the surface and which is like the medium cut quality.

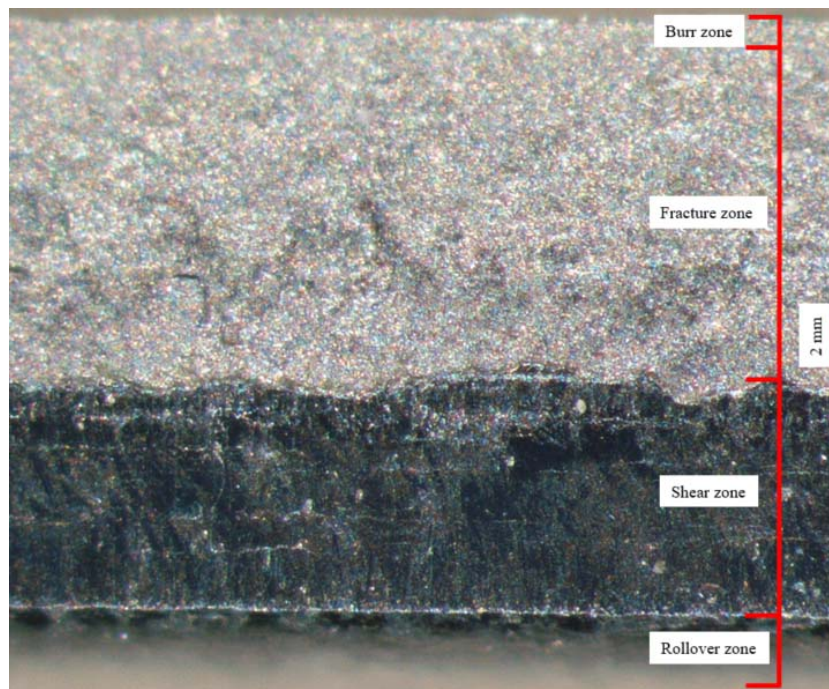


Figure 4.13. The fine cut edge of 2 mm DP600GI specimen from Supplier A.

Figure 4.13 presents the fine cut edge for the 2 mm DP600GI specimen from Supplier A and this edge is a great example of a fine cut edge. The edge constitutes of approx. 35 % shear zone and the burr zone is very small.

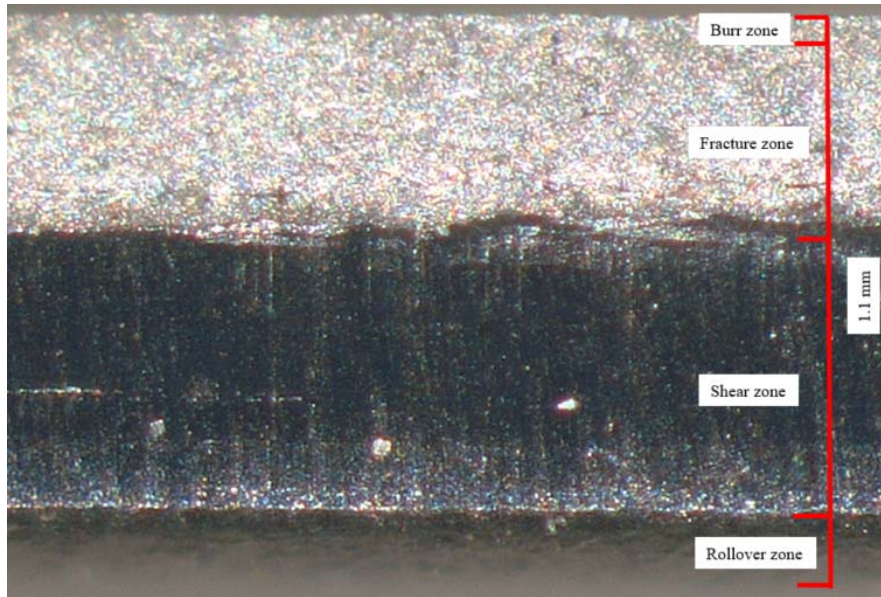


Figure 4.14. The fine cut edge of 1.1 mm DP600UC specimen from Supplier A.

Just as for Figure 4.11 the cut tool adjustments for the fine cut edge seen in Figure 4.14 have not been optimal while performing this cut. The shear zone represents more than 60 % of the edge surface. This will have negative affect of the formability of the specimen.

4.4 Radius measurement of cut tool edges

4.4.1 Worn cut tool

The radius of the worn cut tool was not affected by the cut operation of the test specimens. Thereby, the same cut adjustments have been used for all test specimens.

Before cut operation

Test no.	1	2	3	4	5
Edge radius (μm)	134,77	107,85	107,85	128,56	128,26
Average value	121,45 μm				

Table 4.1. Radius measurement of worn cut tool before cut operations.

After cut operation

Test no.	1	2	3	4	5
Edge radius (μm)	130,81	107,63	117,62	129,27	128,30
Average value	122,73 μm				

Table 4.2. Radius measurement of worn cut tool after cut operations.

4.4.2 Fine cut tool before cut operation

The radius of the fine cut tool was not affected by the cut operation of the test specimens. Thereby, the same cut adjustments have been used for all test specimens.

Before cut operation

Test no.	1	2	3	4	5
Edge radius (μm)	28,79	18,11	20,23	23,63	22,16
Average value	22,58 μm				

Table 4.3. Radius measurement of fine cut tool before cut operations.

After cut operation

Test no.	1	2	3	4	5
Edge radius (μm)	24,51	19,29	19,61	21,55	20,16
Average value	21,02 μm				

Table 4.4. Radius measurement of fine cut tool after cut operations.

4.5 Pre-tests

Types of specimen edges to be used for the experimental tests were:

- 1. **Worn Cut** - Worn tool and 20% clearance
- 2. **Medium Cut** - Fine tool and 20% clearance
- 3. **Fine Cut** - Worn tool and 5% clearance

Both oil and Teflon is necessary to use for the tests to prevent friction between the specimen and punch to affect the fracture limit of the specimen and fracture position.

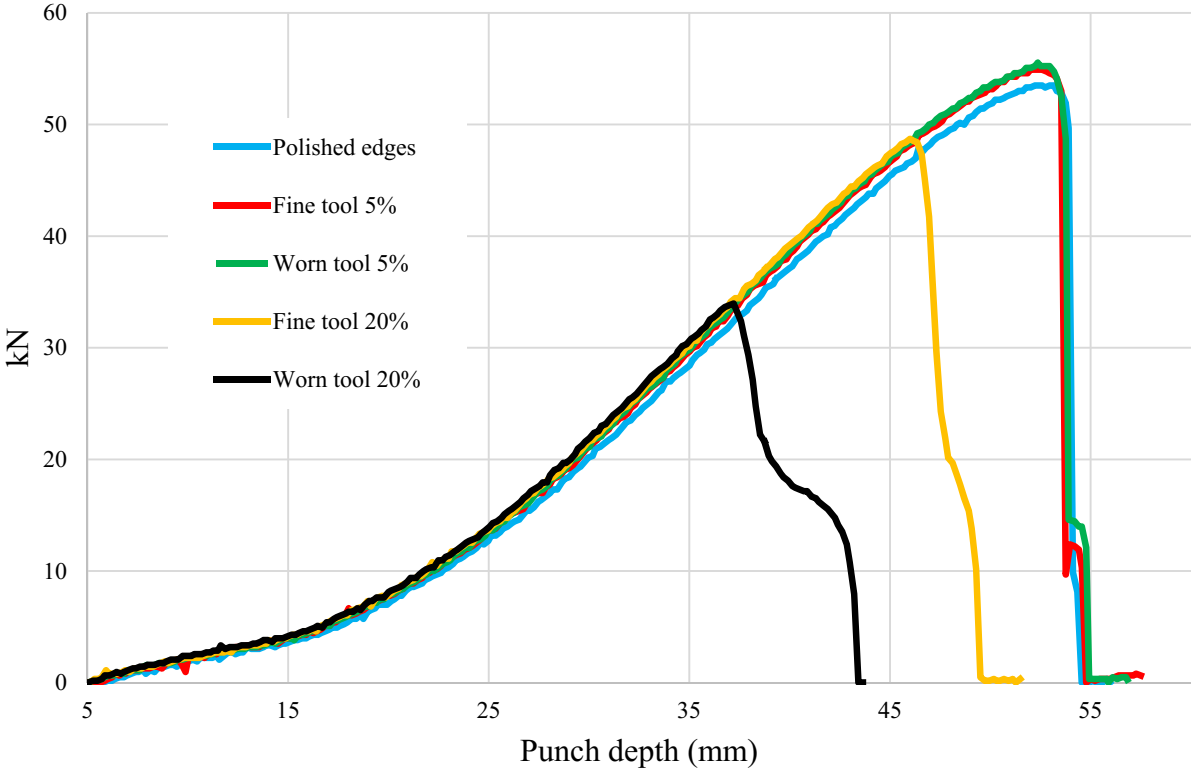


Diagram 4.2. This diagram was used to decide what type of edges of specimens to use in for the experimental tests.

4.6 Influence of rolling direction

The rolling direction of the test specimen had a minor impact on the maximum fracture limit, see Diagram 4.3. Nevertheless, the specimen cut out for the main experimental test had a lengthwise rolling direction (RD).

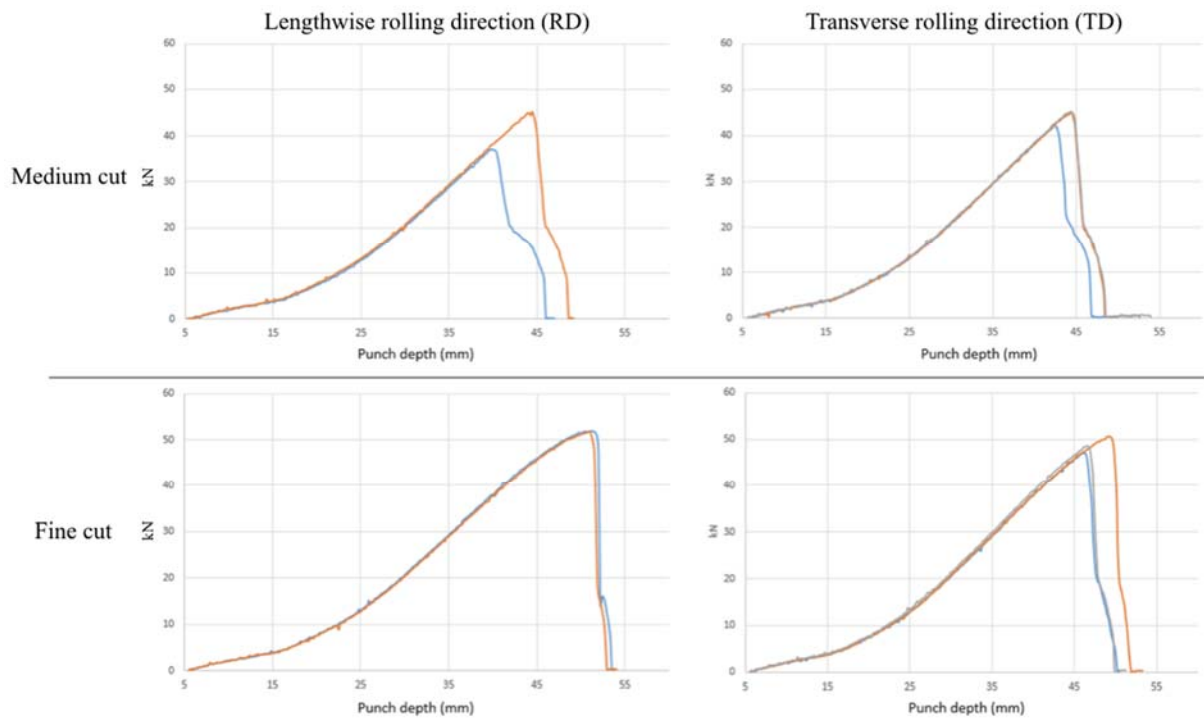


Diagram 4.3. Comparison of values from press operation between rolling and transvers rolling direction.

4.7 Influence of burr zone orientation

With the burr zone facing upwards away from the punch, the fracture limit was exceeded earlier and by a lower applied force and punch depth compared to having the burr zone facing downwards, see Diagram 4.4. Therefore, all main tests were performed with the burr zone facing upwards. The orientation of the burr zone had largest impact on specimens with worn cut edges due to much imperfections and fractures on this type of sheared edge quality.

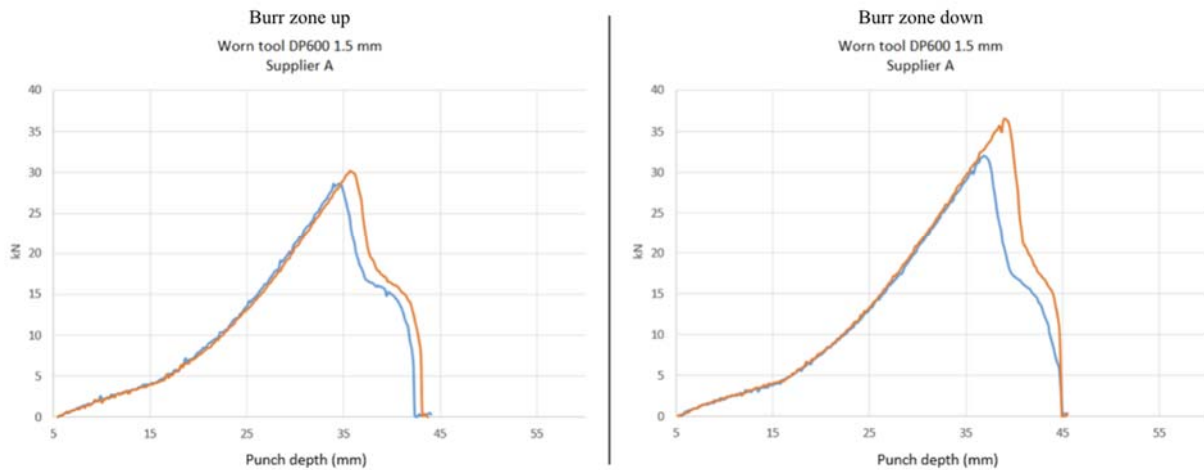


Diagram 4.4. Comparison of results from two specimens with the burr zone facing upwards and two specimens facing downwards. The specimens to the left with the burr zone facing upwards exceed the fracture limit earlier.

4.8 Results from the press experiments

The CTEST punch worked as expected and in 95 of 97 tests the fractures initiated at the sheared (cut) edge of the specimen. All diagram presents minimum punch depth and corresponding punch forces for each material type and cut quality tested. The fracture limit values presented are the lowest value out of two or three press tests per material. The x-axis in the diagrams bellow represents the punch depth in millimeters and the y-axis represents the applied force (kN) of the punch from the stretch forming operation.

4.8.1 DP600GI 1 mm different suppliers

Diagram 4.5 presents that the maximum fracture limit is very similar for all specimens with a worn cut edge and from different suppliers. For the medium and fine edge specimens, a greater variation of the fracture limit can be seen between the three different suppliers. For all material tested the medium cut quality managed to endure higher forces and a deeper punch depth than the fine cut. This trend can be seen for all 1 mm specimens.

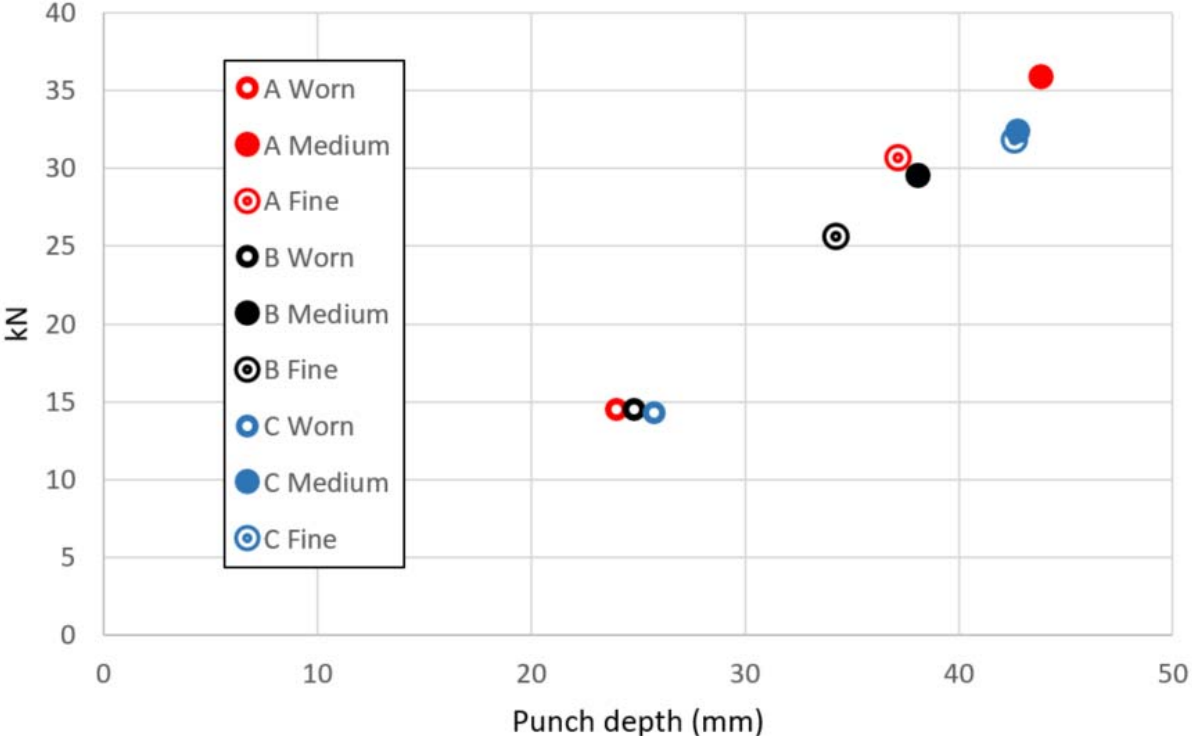


Diagram 4.5. Comparison and result for all DP steels from different suppliers (A, B and C) tested in the press with a thickness of 1 mm.

4.8.2 DP600GI 1.5 mm different suppliers

In the group of materials shown in Diagram 4.6 there are a slightly larger variation within the worn cut specimens than the result shown in Diagram 4.5. This diagram does also present that all three groups of cut qualities does get similar results of maximum fracture strain. The specimens with the worst cut quality manage to endure lowest forces and the medium cut specimens manages to endure higher forces than the worn cut specimens. The specimens with the fine cut quality endured the highest values of maximum fracture strain. For this group of materials with the thickness of 1.5 mm, no specimens with a medium cut quality managed to endure higher fracture strains than a specimen with a fine cut quality.

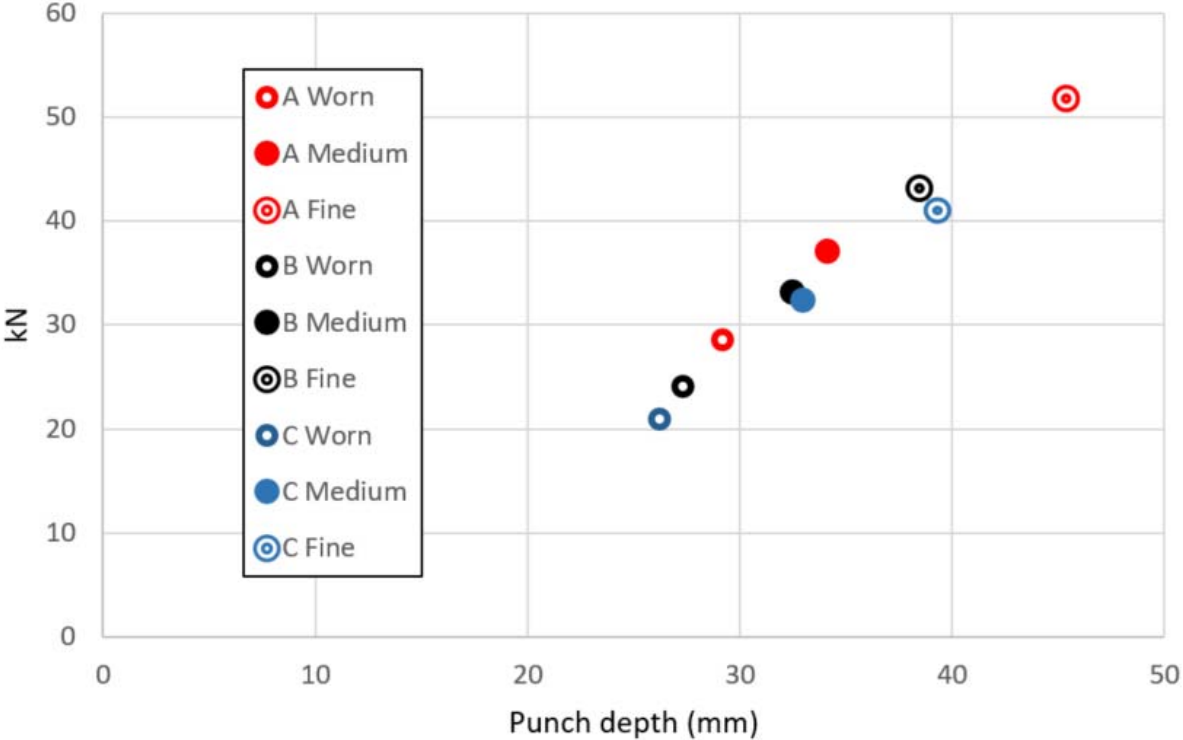


Diagram 4.6. Comparison and result for all DP steels from different suppliers (A, B and C) tested in the press with a thickness of 1.5 mm.

4.8.3 DP600GI 1.5 mm vs. DP600GI 2 mm Supplier A

Specimens with different cut quality made of 2 mm DP600 steel managed to endure higher forces and punch depth than DP600 steel specimens with a thickness of 1.5 mm. For both 1.5 mm and 2 mm specimens the fine cut specimens was the one manage to withstand the highest forces and punch depth, see Diagram 4.7.

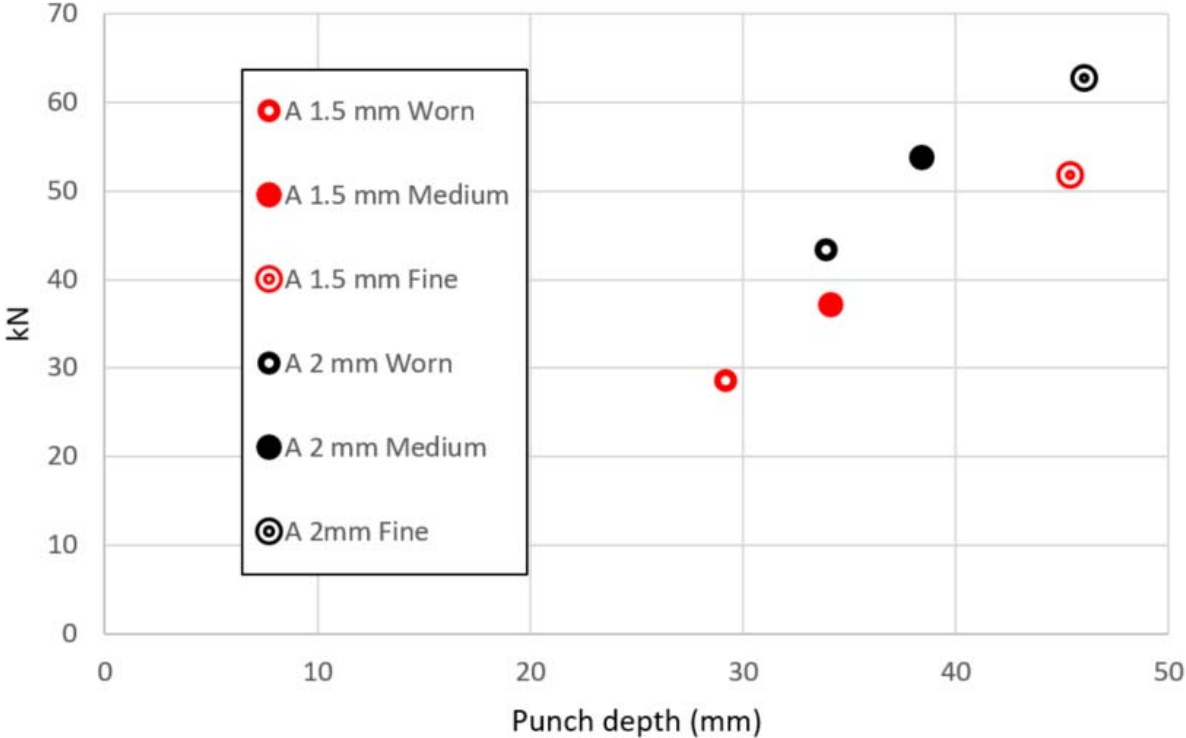


Diagram 4.7. Comparison between specimens made of DP600 1.5 mm and DP600 2 mm from Supplier A tested in the press with different cut qualities.

4.8.4 DP600GI vs. DP600UC Supplier A

Ungalvanized steel managed higher values of the punch force and the punch depth than galvanized steel with similar thickness, see Diagram 4.8. For the ungalvanized steel the specimen with the finest cut endured the highest values of the punch force and punch depth. For the galvanized steel, it was instead the medium cut specimen that managed to endure the highest strain.

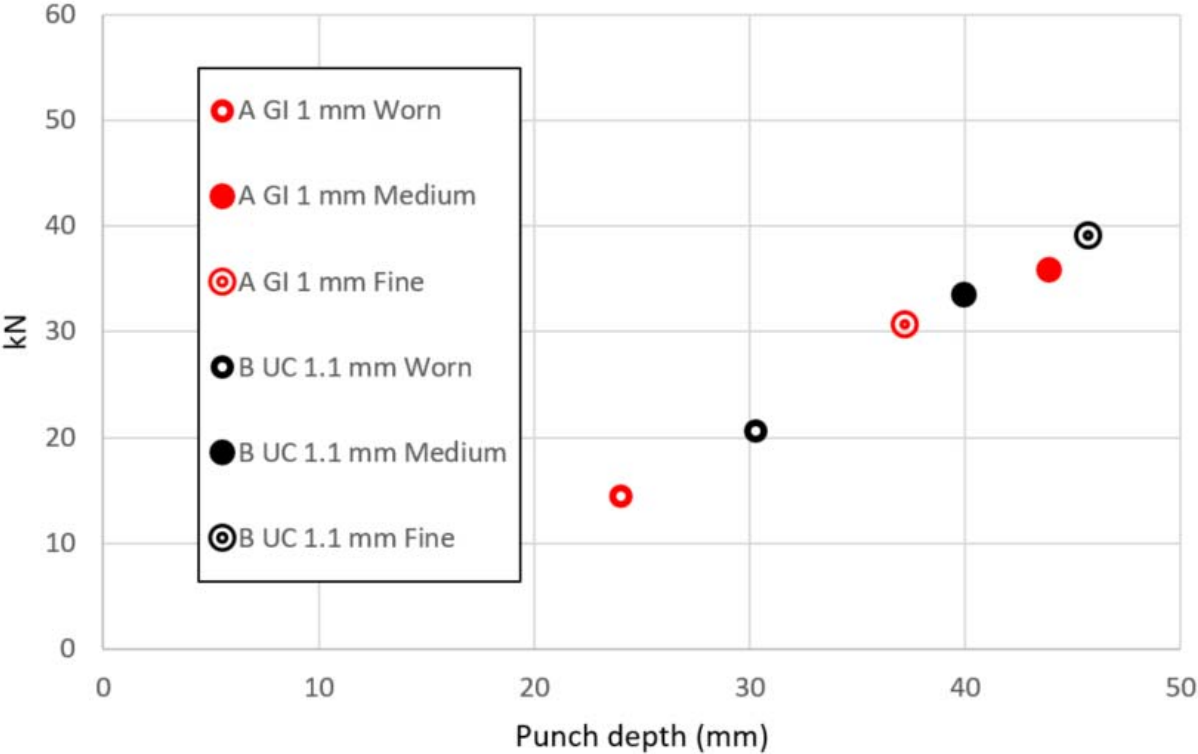


Diagram 4.8. Comparison between DP600GI and DP600UC from Supplier A tested in the press with a thickness of 1 mm and 1,1 mm and different cut qualities.

4.8.5 DP600GI 1 mm vs. DP800GI 1 mm Supplier B

Specimens made of DP600 steel and with a thickness of 1 mm, generally managed to endure a deeper punch depth but lower press forces than specimens made of DP800 with the same thickness. For both DP600 and DP800 specimens with the thickness of 1 mm, the highest strain was achieved with the medium cut specimens, see Diagram 4.9.

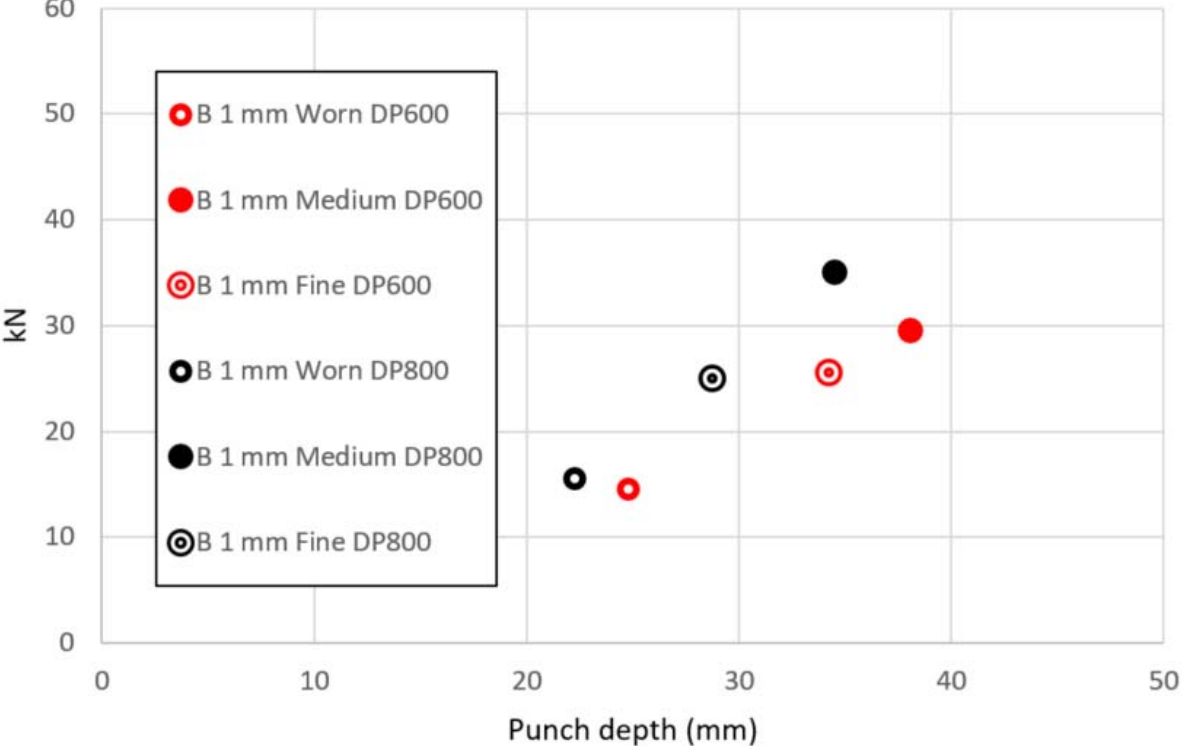


Diagram 4.9. Comparison between specimens made of DP600 1 mm and DP800 1 mm from Supplier B tested in the press with different cut qualities.

4.8.6 DP600GI 1.5 mm vs. DP800GI 1.5 mm Supplier B

Specimens made of DP600 steel with a thickness of 1.5 mm, generally managed to endure a deeper punch depth and similar or higher punch force values than specimens made of DP800 with the same thickness. With a specimen thickness of 1.5 mm, the highest strain value was achieved with the fine cut specimen both for DP600GI specimens and DP800 GI specimens, see Diagram 4.10.

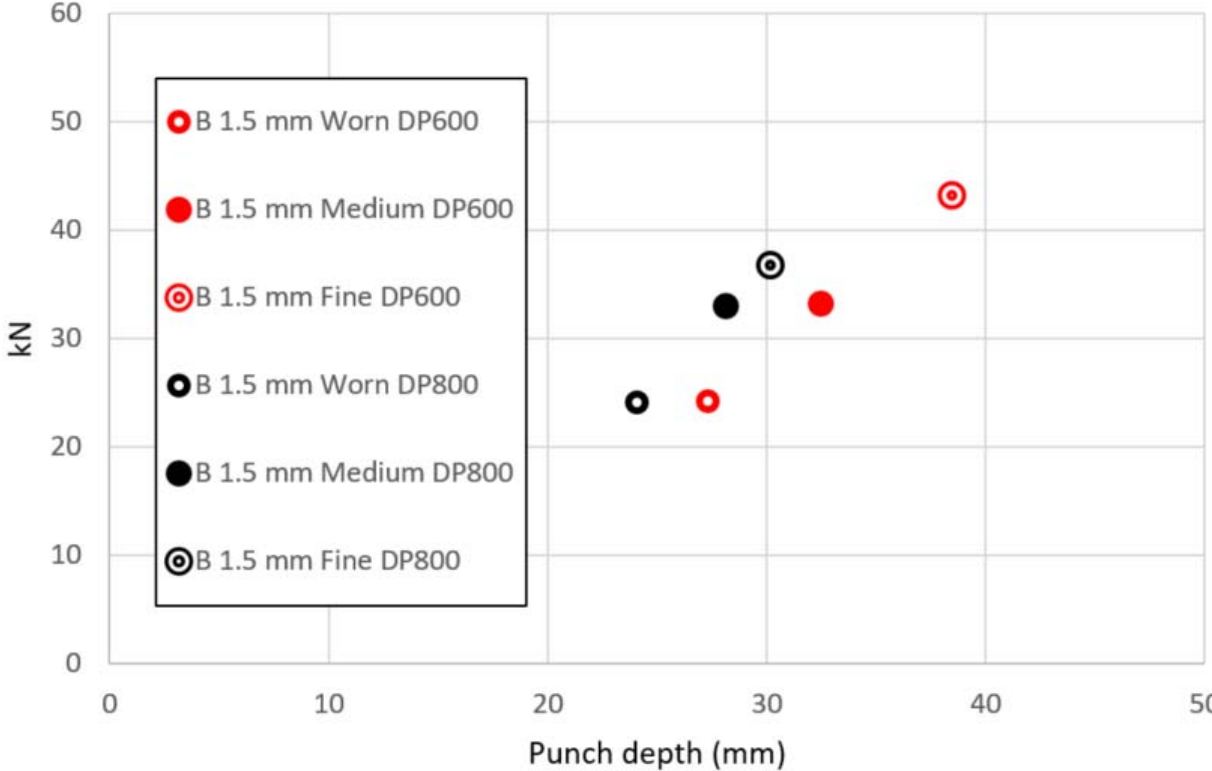


Diagram 4.10. Comparison between specimens made of DP600 1.5 mm and DP800 1.5 mm from Supplier B tested in the press with different cut qualities

4.9 Evaluation of press experiments in ARAMIS

The results from ARAMIS are presented for the 1.5 mm DP600GI steel from Supplier A. Small fractures appear in the sheared edge of the specimens just before maximum punch depth is reached, see Diagram 4.11. When maximum punch depth is reached one of these small fractures grow very fast and the specimen is split in two parts. However, small fractures already appear in the sheared edge before maximum punch depth is reached, especially for worn and medium cut specimens.

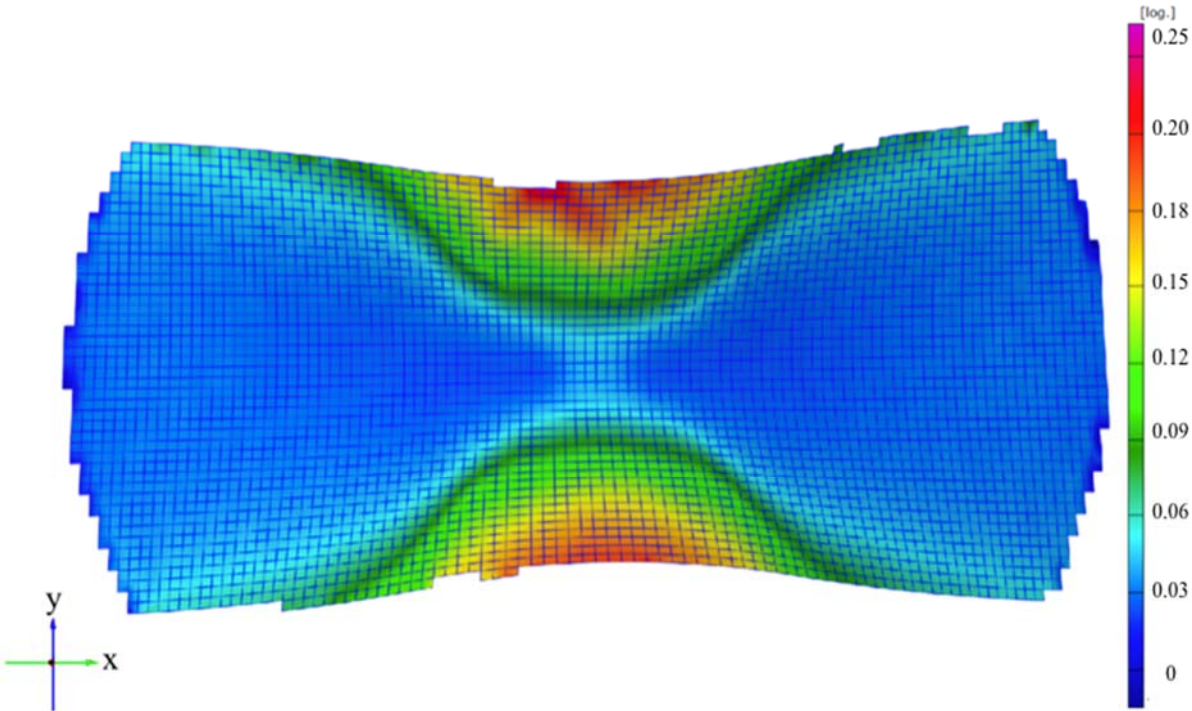


Figure 4.15. The Major strain from ARAMIS just before a large fracture appear. The top edge represents the cut edge. Maximum fracture strain is 0.25.

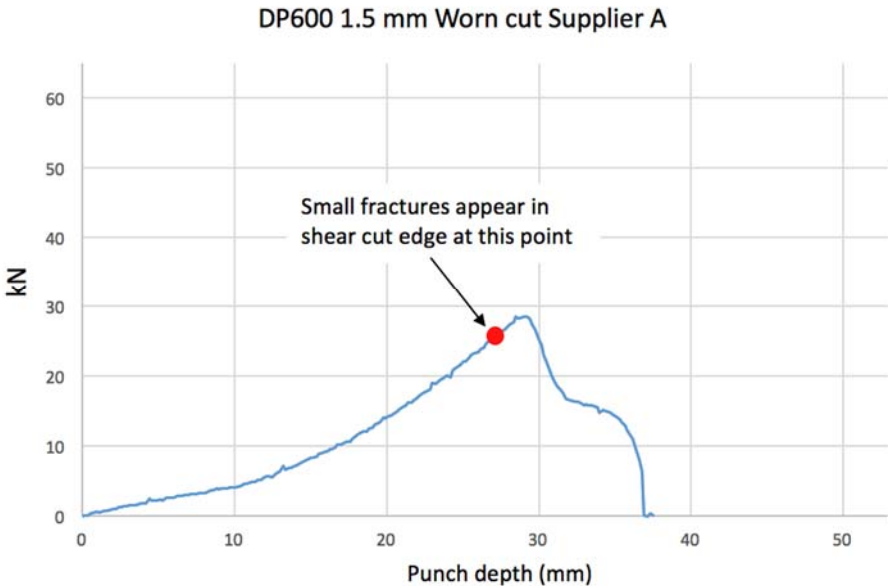


Diagram 4.11. Small fractures appear in the sheared edge of the specimen before maximum force and punch depth is reached and the specimen split into two parts.

4.10 Comparison of simulation in AutoForm vs. ARAMIS DIC system

4.10.1 Comparison of geometry of simulations and ARAMIS DIC system

The results show the comparison with material no. 5, see table 3.1. The comparison of the simulation and real test demonstrated similar displacements for all material tested. Figure 4.12 presents the displacement in millimeters between the simulated geometry in AutoForm and the real specimen geometry from the press test.

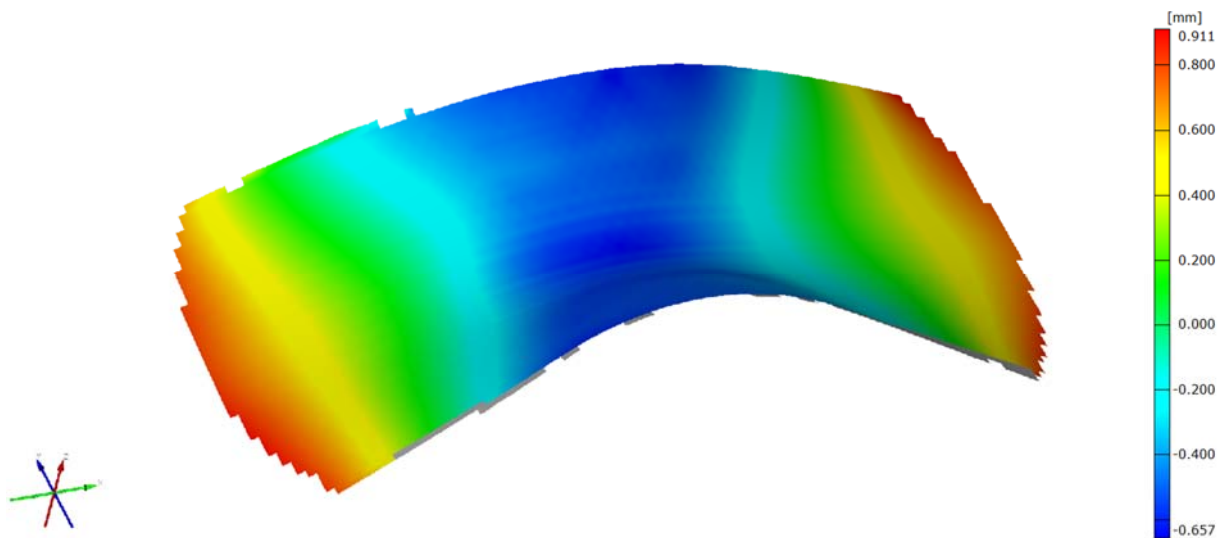


Figure 4.16. The displacement in mm between the simulated geometry of the specimen in AutoForm and the real geometry of the test specimen generated in ARAMIS. This is the displacement value from material no. 5.

4.10.2 At maximum punch force and punch depth

At maximum punch force and punch depth the strain is evenly distributed on the edge of the specimen in the simulation in AutoForm, see Figure 4.17. At maximum punch force and punch depth in the result from ARAMIS the strain is concentrated to one of the already existing small fractures, see Figure 4.18. Both Figure 4.17 and 4.18 represents the extreme values at the maximum point of the punch force vs. punch depth curve just before the specimen is split in two parts, see Diagram 4.12.

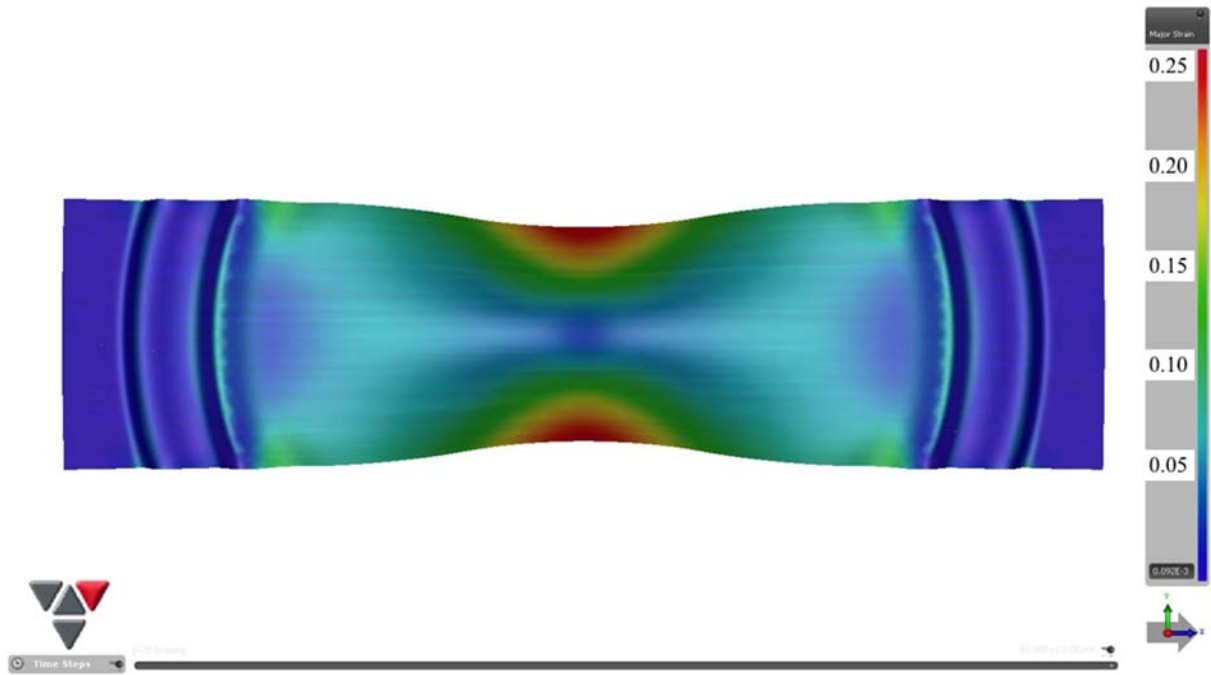


Figure 4.17. The major strain value of the sheared cut edge in the simulation in AutoForm at maximum press depth and force before the large fracture appear that will separate the specimen. See diagram 4.13 to see the point in the forming curve.

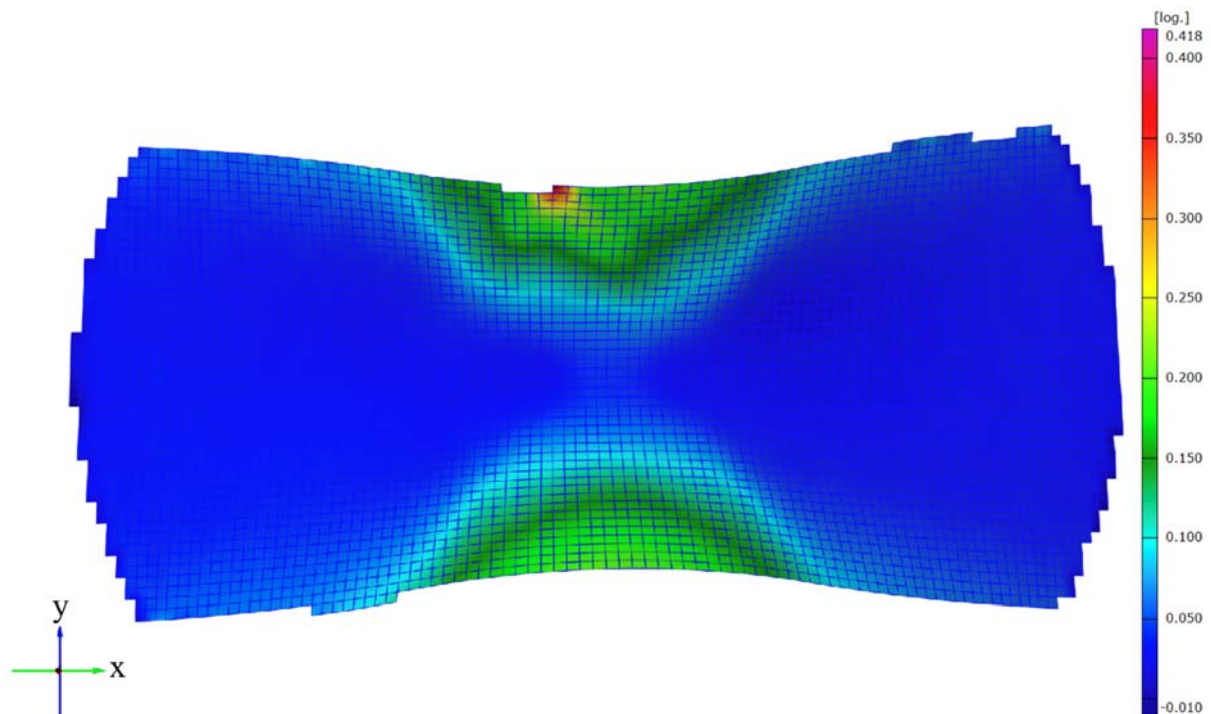


Figure 4.18. The strain at the fracture when maximum force and punch depth is reached just before the fracture grow and separates the specimen. See diagram 4.13 to see the point in the forming curve.



Diagram 4.12. The point where maximum force and punch depth is reached. Small fractures have already appeared at the sheared cut edge in this point and one of them will grow bigger and separate the specimen. This phenomenon was only seen from the results in ARAMIS.

4.10.3 Punch force vs. punch depth curve

The variation of the values from the simulation in AutoForm and the press test for material no. 5, see table 3.1, with a worn cut is presented in figure 4.13. Both curves follow a similar trend which is very positive. Further adjustments of the maximum true strain value in AutoForm can be done to obtain more matching values between AutoForm and press tests. The value from the simulation show a slightly higher value of the fracture strain than the value from the press test.

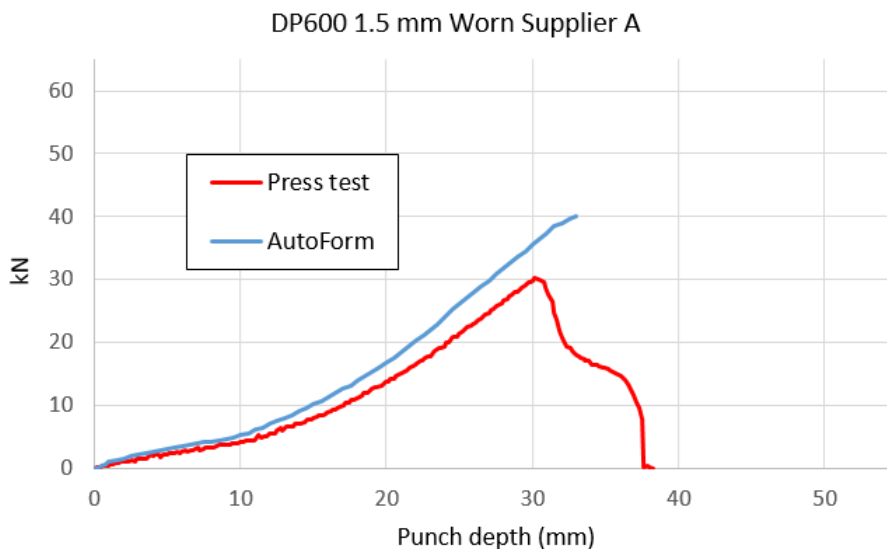


Diagram 4.13. Comparison between the values from the simulation in AutoForm and the press test. This figure presents the comparison for material no. 5 with a worn cut.

4.10.4 New values of maximum fracture strain for simulations in AutoForm

The new fracture limit values for each cut quality generated in AutoForm are presented in Table 4.5 below.

Material type	Thickness (mm)	Supplier	Worn cut (ϵ)	Medium cut (ϵ)	Fine cut (ϵ)
DP600 GI	1.0	A	0.19	0.60	0.41
DP600 GI	1.5	A	0.26	0.33	0.54
DP600 GI	2.0	A	0.24	0.29	0.32
DP600 UC	1.1	A	0.29	0.38	0.66
DP600 GI	1.0	B	0.21	0.38	0.31
DP600 GI	1.5	B	0.23	0.30	0.36
DP800 GI	1.0	B	0.16	0.41	0.30
DP800 GI	1.5	B	0.18	0.25	0.28
DP600 GI	1.0	C	0.19	0.46	0.43
DP600 GI	1.5	C	0.20	0.29	0.37

Table 4.5. All new values of the true strain (ϵ) for all types of material and cut qualities simulated in AutoForm.

5 DISCUSSION

5.1 Design of the punch geometry

The design of the punch did concentrate the strain to the edges of a test specimen. In 98 % of the tests performed in the press the fracture started from the trim edge of the specimen. For the two tests where the fracture started from the polished edge it could have been some imperfections or dents on the polished edge, allowing the fracture to initiate by a lower applied force or strain of the material.

In a comparison between the CTEST and a tensile test, the tensile test does not consider the orientation of a cut edge and if the burr zone is facing in any direction. As shown in Diagram 4.4, the orientation of the burr zone has an impact to maximum fracture strain of the edge. The CTEST does consider the orientation of the burr zone and can measure extreme values for maximum strain depending on the orientation of the burr zone. Therefore, an ordinary tensile test is not as suitable as CTEST for testing of trim edges that later will be stretched.

5.2 Tensile tests

One of the reasons to perform tensile tests of all materials in an early phase of the study was to explore if a variation was noticeable between specimens with a cut and a polished edge. The result showed that it was a clear difference between a trimmed and a polished edge and that the polished edge had higher values of the strain before fracture. However, the tensile test does not consider the orientation of the burr zone and how the burr zone affects the formability of an edge. Therefore, it was interesting to make further tests using the CTEST method.

5.3 Cut edges of specimens

A large variation between the three cut qualities could be seen from the microscopic pictures comparing each cut edge quality.

5.3.1 Worn cut - worn tool and 20 % clearance

One characteristic found for all worn cut edges was the large shear zone and burr zone relative the thickness of the material. The transition between the shear zone and fracture zone is uneven and dents and imperfections exists on the surface of the shear zone. These imperfections have a negative impact on the formability of the edge during stretch forming. All worn cut edges have a big burr zone, consisting imperfections and small micro cracks. These micro cracks are a perfect starting point for a fracture.

The worn cut edge for the 1.1 mm DP600UC steel is presented in figure 4.6. This edge must have been exceeded for work hardening of the material in the edge because of the large shear zone due to the worn cut tool.

5.3.2 Medium cut - fine tool and 20 % clearance

The edge surfaces of all medium cut edges consisted approx. of 25-30 % by the shear zone. No large variation of the cut edge zones was found for this quality. This means that good adjustments of the cut tool have been used to cut out the medium cut edges. The burr zone for the medium cut edges are not as big as for the worn cut edges. Therefore, not as many micro cracks can be found in the medium cut edges.

5.3.3 Fine cut - worn tool and 5 % clearance

The adjustments were not optimal for the fine cut 1 mm steel specimens. The shear zone was too large and therefore these edges will not manage to endure as high punch depth as the medium cut edges with the same thickness. To cut out 1 mm specimens with a fine cut the fine edge cut tool could be used instead of the worn edge cut tool that was used for the specimens in this study. Therefore, same cut tool could not be used to cut out a fine edge of 1 mm and 1.5 mm DP steel specimens.

For 1.5 mm and 2 mm specimens edges the result was much better and these edges can be defined as fine cuts. Therefore, the formability of these edges were better than the medium cut edges with the same thickness.

5.4 Radius measurement of cutting tool edges

This measurement was done to bely that the radius of the two different cut tools wasn't affected or changed from cutting out the series of specimen used for the press experiments. This means that all specimen edges have been cut out during the same conditions.

5.5 Pre-tests

The punch was manufactured in a milling machine and the contact surface of the punch between the punch and specimen was not processed or polished after milling. The contact surface of the punch could have an impact of the friction between the punch and specimen. Therefore, the surface could be polished for future tests with the punch to lower the friction even more.

After the pre-tests when evaluating the result, the result was very similar between polished, 5 % clearance with a fine tool and 5 % clearance with a worn tool. The reason to choose the quality 5 % clearance with a worn tool out of these three, was because this was the one most likely to be used during manufacturing and stamping in the production at Volvo Cars.

5.6 Influence of rolling direction

Earlier research [13] explain that specimen with TD rolling direction is slightly more sensitive for fractures and does endure lower strain. The pre-test showed that there were no great differences in maximum fracture strain between RD and TD specimen. For medium cut specimen, the RD specimen endured lower values of force and punch depth before fracture than TD specimen. For specimen with a fine cut it was instead the TD specimen that did break at a lower force and punch depth than RD specimen. Because of these small variations only specimen with a RD rolling direction were prepared for the experimental tests.

5.7 Influence of burr zone orientation

The orientation of the burr zone of the cut edge of the specimen had a large impact on the maximum fracture strain of the specimens tested during the pre-tests. With the burr zone facing upwards from the punch the specimen did break at an earlier stage than with the burr zone facing towards the punch. The reason to this phenomenon, with the burr zone facing upwards, is that the imperfections or fractures on the burr zone will grow when the burr zone edge is stretched out. With the burr zone facing down against the punch, it is instead the rollover zone that will be stretched out and the rollover zone does not contain as many imperfections and micro cracks as the burr zone.

5.8 Results from the press experiments

5.8.1 DP600GI 1 mm thick from different suppliers

From the results presented for this group of edge quality and thickness the medium cut edges managed to endure highest punch depth and force. This supports the statement presented in chapter 5.3.3, that the settings of the cut tool used to cut out the 1 mm specimen was not correct or optimal. The worn cut tool with a 122 μm edge radius and a clearance of 5 % was used to cut out the fine edges. These adjustments of the cut tool were not optimal for cut out a fine edge of the 1 mm steel.

5.8.2 DP600GI 1.5 mm thick from different suppliers

The results from this group of specimens tested did follow the expected outcome. The specimen with the worst cut did break in an earlier phase than the medium and fine cut specimen. The specimen with the finest cut were the most durable and managed to endure the highest forces and punch depth. This trend could be seen for all specimen from different suppliers. Although, the endurance did vary between the specimens from different suppliers. Within all 1.5 mm thick DP600GI specimens with different cut qualities, specimens from supplier A was the ones to endure the highest forces and punch depth.

5.8.3 DP600GI 1.5 mm thick vs. DP600GI 2 mm thick Supplier A

The 2 mm specimen managed to endure higher values of the force and strain than the 1.5 mm specimen and this was the expected outcome from this comparison. An increase of the thickness will also lead to an increase in force.

5.8.4 DP600GI vs. DP600UC Supplier A

According to [19] the galvanization process of a steel has a negative impact of the strength of the steel. This explains the trend and variation between galvanized and ungalvanized DP600 steel presented in diagram 4.8. The variation of 0.1 mm in thickness for the GI and UC steel does have a positive impact of the strength of the UC steel. Nevertheless, the higher strength of the UC steel cannot just depend on the slightly higher thickness. Undoubtedly, DP600UC steel have greater formability than DP600GI steel.

5.8.5 DP600GI 1 mm thick vs. DP800GI 1 mm thick Supplier B

In this comparison presented in figure 4.9, the medium cut quality specimens has a larger formability than the fine cut DP600 and DP800 specimens. This trend has been seen for all 1 mm DP steels tested in this study. The outcome from this comparison was therefore expected. The stronger DP800 steel endures higher values of the force but not as high punch depths as the DP600 steel and therefore, DP600 have higher formability than DP800.

5.8.6 DP600GI 1.5 mm thick vs. DP800GI 1.5 mm thick Supplier B

Same characteristics is shown in diagram 4.9 as in 4.10 when comparing DP600 and DP800. The DP600 steel endures higher punch depths and the DP800 endures higher forces due to a higher tensile strength. One divergent result could be found in comparison between the 1.5 mm DP steels. The fine cut specimen of DP600 endured not only highest strain but also the highest value of force compared to DP800 specimen with the same cut quality.

5.9 Evaluation of press experiments in ARAMIS

For the worn and medium cut specimen analyzed in ARAMIS it was clear that it was more than one small fracture that appeared before maximum force and punch depth was reached. Also by a visual inspection of a specimen tested in the press small fractures can be seen in the sheared edge with the worn and medium cut quality. Therefore, during stretch forming of specimen with worn and medium cut qualities, small fractures may occur when the specimen is stretched to maximum strain. If small fractures are not wanted from a stretch forming operation, a slightly lower value of the strain needs to be used in the simulation for specimen with worn and medium cut quality of the edges.

5.10 Comparison of simulation in AutoForm vs. ARAMIS DIC system

5.10.1 Comparison of geometry of simulations and ARAMIS DIC system

The small difference between the simulated geometry and the geometry from the press test (ARAMIS) means that AutoForm uses a correct geometry of the simulated specimen when performing the simulations, see Figure 4.16. If big displacements (several millimeters) were discovered, then it would be necessary to adjust the geometry in AutoForm. This operation was performed to determine that AutoForm used the correct geometry.

5.10.2 At maximum punch force and punch depth

When comparing the strain concentrations between the simulation in AutoForm, see Figure 4.17, and the result from ARAMIS, see Figure 4.18, a severe difference could be seen at maximum force and punch depth for the specimens tested. A concentration of the strain is seen at the growing fracture in ARAMIS at maximum punch force and punch depth. In the simulation the strain is still evenly distributed around the edge of the specimen at the same values of punch force and punch depth and the strain concentration phenomenon cannot be seen as in ARAMIS. Therefore, the simulation in AutoForm does not include these strain concentrations in small fractures at the point just before one of the fractures grow larger and separates the specimen.

5.10.3 Punch force vs. punch depth curve

Diagram 4.11 shows that the punch force vs. punch depth curve values from the simulation follow a similar trend as the values from the press tests (ARAMIS). Optimal would be if these values showed the exact same trend. The values of the true strain can be further adjusted in AutoForm to make the values match even more.

Furthermore, what not should be forgotten is that the values of the forces and punch depth from the press test is measured with sensors in the press. The settings and adjustments of these sensors may not have been optimal and this can be one cause to the variation seen in Diagram 4.13. However, the exact same sensors were used in the press for all press tests and therefore this variation between force and displacement values is seen for all types of materials.

5.10.4 New values of maximum fracture strain for simulations in AutoForm

All values of the true strain generated by the simulations in AutoForm will be useful for Volvo Cars when determining the formability during stretch forming of a DP steel with a certain cut quality. Volvo Cars will now know the characteristics for each shear cut quality tested in this study and can therefore prevent fractures to appear and have a more reliable production. Unfortunately, the values of 1 mm fine cut specimen will not represent a real fine cut due to wrong adjustments of the cut tool and cannot be used without a risk of fractures.

As presented in Diagram 4.4 the orientation of the burr zone does affect the formability of a specimen or blank. When setting the data and inputs before performing a simulation in AutoForm there exists no option to define the orientation of the burr zone. The existing version of AutoForm does not consider the orientation of the burr zone in the calculation. For future versions of AutoForm this would probably be an important variable and input to add to the simulation, especially for worn cut edges with big burr zones.

6 CONCLUSIONS

A new punch (CTEST, Concentrated Trim Edge Strain Test) have been developed that concentrates the strain to the shear cut edges of a specimen in a press test. The new CTEST method does consider the orientation of the burr zone of a shear cut edge which an ordinary dog bone tensile test does not. Different types of Dual-Phase (DP) steel specimens with different thickness and quality of shear cut edges have been tested using the new CTEST punch. These tests were performed to determine how three different shear cut edge qualities (fine cut, medium cut and worn cut) of specimens affects the fracture strain and the formability of the edges. Types of DP steels tested are DP600GI, DP600UC and DP800GI from three different suppliers.

Undoubtedly, the quality of a shear cut edge have a large impact of the formability and maximum fracture strain of a test specimen. A worn cut quality specimen does have lower formability and manages to endure lower fracture strain than a specimen with a medium or fine edge cut quality. The rolling direction of a shear cut specimen does have a minor affect to the formability and fracture strain of the specimen. Specimens made of DP800GI steel does have a lower formability than DP600GI specimens for all qualities and thickness compared in this study.

The adjustments of the cut tool used to cut out 1 mm thick specimens with a fine cut was not optimal and therefore the medium cut quality with the same thickness had higher formability in this study. Better adjustments were used to cut out 1.5 mm and 2 mm specimens of all cut qualities. For all 1.5 mm and 2 mm specimens tested it were the fine cut specimens that had the highest formability and endured highest values of the force and punch depth. 2 mm specimens had higher formability than 1.5 mm specimens.

The uncoated DP600UC steel specimen with a thickness of 1.1 mm had higher formability and endured higher values of the fracture strain for all three types of cut qualities compared to 1 mm galvanized DP600GI steel. Despite poor adjustments of the cut tool used to cut out the fine cut edge of the 1.1 mm DP600 UC steel specimens, this quality had the highest formability.

The orientation of the burr zone has impact on the formability to a specimen. With the burr zone facing upwards relative the CTEST punch the formability of the specimen is decreased compared to a test with burr zone facing downwards, especially for a worn cut specimen with a lot of imperfections and micro cracks on the edge. For an upwardly facing burr zone the micro cracks will be stretched out and therefore the formability will be lower than with a downwardly facing burr zone.

The analyze in ARAMIS unveiled that several small fractures appear in specimen's shear cut edge just before maximum punch force and punch depth is reached in the press. At maximum punch force and punch depth one of these small fractures grow quickly and the specimen is split in two parts. This phenomenon was seen for specimens with a worn and medium cut quality edge.

The simulation in AutoForm does show a slightly higher value of the punch force than the value from the press test. The simulation does not show values that exactly match to the maximum fracture strain values from the real tests and further adjustments of the input values has to be done in AutoForm. This shows the importance of performing real tests to validate values from the simulations.

7 RECOMMENDATIONS AND FUTURE WORK

In this study, specimen with a shear cut edge parallel with the rolling direction (RD) was used for the press test. A future study can be done to determine the impact of different rolling directions more in detail. The study could also determine the optimal adjustments of the rolling direction during stretch forming and sheet metal forming.

A future study can be performed with a polished surface of the CTEST punch to lower the friction between the specimen and punch. This tests would be performed without using oil and Teflon to lower the friction and would therefore match the settings used in the production at Volvo Cars better.

Other materials such as aluminum could be tested using the CTEST method. Fractures may also appear in cut edges of aluminum specimen during sheet metal forming and the same type of tests could be performed as in this study. A deeper study of the variation in formability of GI and UC steel can be done. This study could include GI and UC steel from different suppliers and with different thickness and rolling direction.

Specimen cut out using other types of cut methods could be analyzed using the CTEST method. Examples of other cut methods could be laser cut and water cut. The impact of work hardening on the formability could be studied for shear cut edges with different qualities.

The test series with 1 mm DP600GI and 1.1 mm DP600UC specimens could be performed again with optimal adjustments to the cut tool used to cut out the fine cut quality. This could be performed to achieve even more reliable results within this group of DP steels tested.

8 REFERENCES

- [1] A.K. Skiöld, “Olofström; industrisamhälle och integrationsort,” Länsstyrelsen Blekinge län, Olofström, Sweden, 1th ed., 2005.
- [2] (2017, Jan. 3). *AutoForm Solution Overview* [Online]. Available: <http://www.autoform.com/en/products/solution-overview/>
- [3] M. Sarwar, R. Priestner, “Influence of ferrite-martensite microstructural morphology on tensile properties of DP steel,” in *Journal of material science 31*, pp. 2091-2095, 1996.
- [4] *Product information for DP steels*, version 0, Thyssenkrupp Steels Europe AG, Duisburg, Germany, April 2016.
- [5] H. Föll (2016). Overview of Major Steels (1th ed.) [Online]. Available: http://www.tf.uni-kiel.de/matwis/amat/iss/kap_9/advanced/t9_2_1b.html
- [6] L. Hågeryd, *et al.*, “Klippande bearbetning,” in *Modern produktionsteknik del 1*, 2nd ed., Stockholm, Sweden: Liber, 2002, pp. 176-206.
- [7] N. E. Dowling, “Mechanical Testing: Tension Test and Other Basic Tests,” in *Mechanical Behavior of Materials*, 4th ed., Harlow, England: Pearson Education Limited, 2013, pp. 157-161.
- [8] F. Birath, A. Nilsson, “Topology optimization of a stamping die,” M.S. thesis, Div. of Solid Mech., Lund Univ., Lund, Sweden, 2006.
- [9] N. E. Dowling, “Mechanical Testing: Tension Test and Other Basic Tests,” in *Mechanical Behavior of Materials*, 4th ed., Harlow, England: Pearson Education Limited, 2013, pp. 123-128.
- [10] L. Hågeryd, *et al.*, “Klippande bearbetning,” in *Modern produktionsteknik del 1*, 2nd ed., Stockholm, Sweden: Liber, 2002, pp. 95-97.
- [11] *Software Solutions for Sheet Metal Forming*, version 1, AutoForm Engineering GmbH, Switzerland, 2016.
- [12] (2017, Jan. 5). *ARAMIS - 3D Motion and Deformation Sensor* [Online]. Available: <http://www.gom.com/metrology-systems/aramis.html>
- [13] Q. Li, *et al.*, “Research difference if strain distribution and microstructure evolving between rolling direction and transverse direction of AM50 Mg alloy plate by digital image correlation,” in *Advances in Materials Science and Engineering*, vol. 2015, Article ID 175873, 7 pages, 2015.
- [14] N. E. Dowling, “A Survey of Engineering Materials: Alloying and Processing of Materials,” in *Mechanical Behavior of Materials*, 4th ed., Harlow, England: Pearson Education Limited, 2013, pp. 68-69.
- [15] J. Carpio, *et al.*, “Environmental factors in failure during structural steel hot-dip galvanizing,” in *Engineering Failure Analysis*, vol. 16, March 2009, pp. 585-595, and presented at the 24th meeting of the Spanish Fracture Group, Burgos, Spain, March 2007.
- [16] E. Atzema, P. Seda, “Sheared edge tensile test improved: SETi,” presented at the Forming Tech. Forum, Zurich, Switzerland, June 2015.
- [17] W. Volk, *et al.*, “Advanced failure prediction in sheet metal forming,” presented at the Forming Tech. Forum, Zurich, Switzerland, June 2015.
- [18] Z.K. Teng, X.M. Chen, “Edge cracking mechanism in two DP advances high strength steels,” *Materials Science & Engineering*, Michigan, USA, pp. 645-653, 2014.
- [19] X. Zhuang, *et al.*, “Failure mode and ductility of dual phase steel with edge crack,” presented at the 11th Int. Conf. on Technology of Plasticity, Nagoya, Japan, October 2014.
- [20] K. Wiegand, “Existing possibilities to predict edge cracks in the sheet metal forming simulation”, Presentation at IDDRG2016, Graz, Austria, 2016.
- [21] (2017, Jan. 9). *Discover Catia* [Online]. Available: <http://www.3ds.com/products-services/catia/>

APPENDIX A

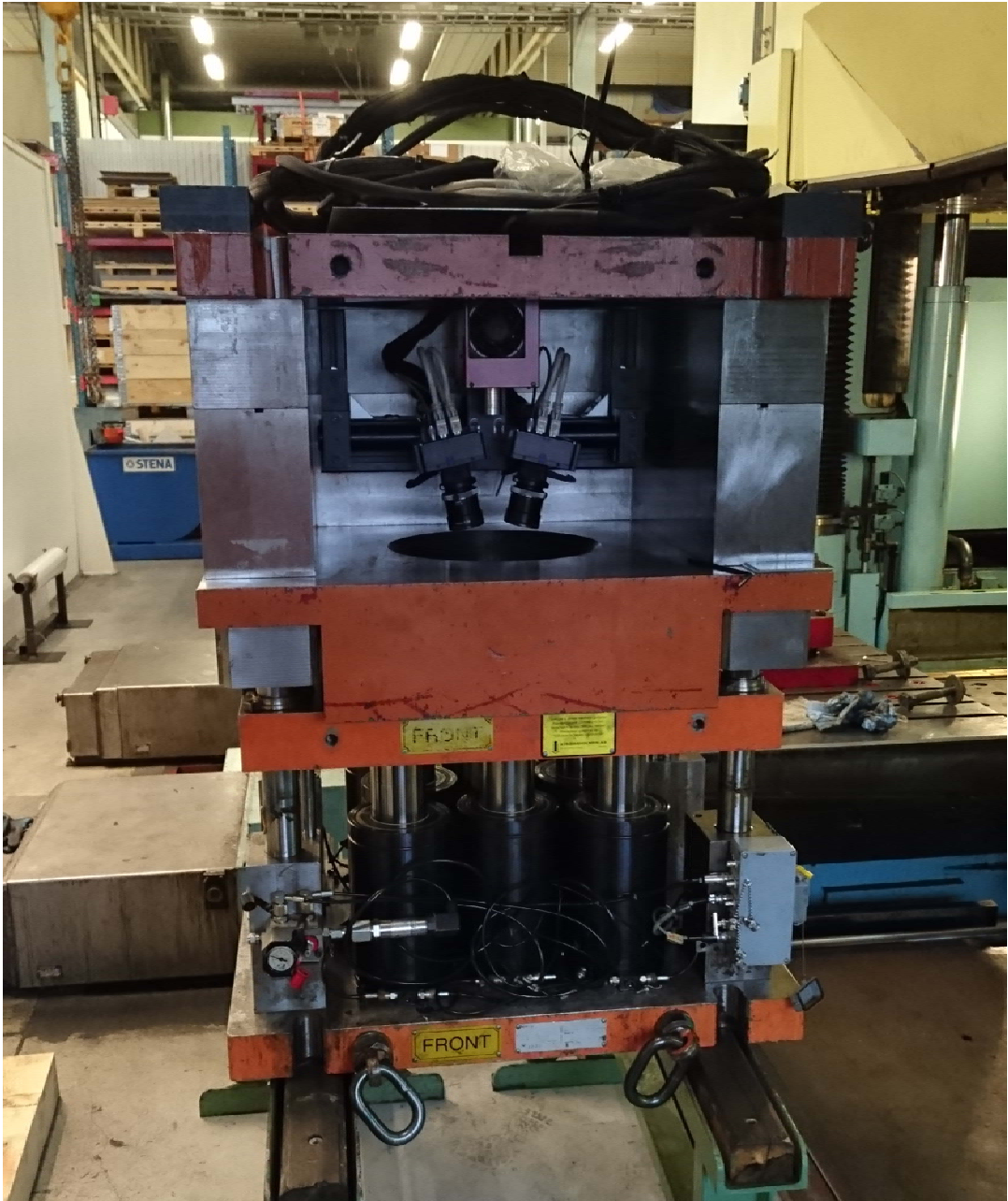


Figure A.1. This was the press tool used during the press tests. The new punch design (CTEST) was installed in this tool. The two ARAMIS cameras can be seen in the middle.

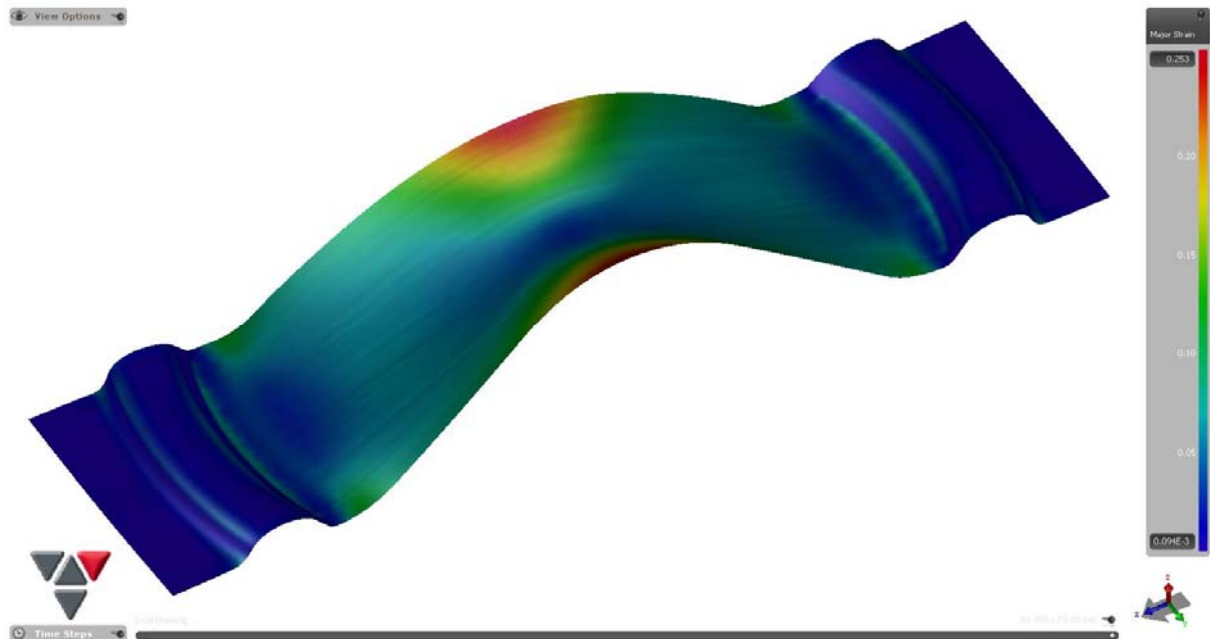


Figure A.2. The major strain distribution for specimen after simulation in AutoForm using the CTEST punch.

